AN EXPERIMENTAL STUDY OF THE EFFECT OF ANISOTROPICAL CONSOLIDATION ON THE COHESION AND FRICTION IN SATURATED CLAY

By

John Russell Hall, Jr.

A Thesis Presented to the Graduate Council of the University of Florida in Partial Fulfillment of the Requirements for the Degree of Master of Science.

UNIVERSITY OF FLORIDA

June, 1960

ACKNOWLEDGMENTS

The writer wishes to extend his appreciation to all those persons who contributed suggestions for the research and writing of this thesis.

The writer is particularly indebted to Professor John H. Schmertmann for his guidance and many suggestions throughout the entire investigation and writing of this thesis.

TABLE OF CONTENTS

LIST OF TABLES

LIST OF FIGURES

LIST OF SYMBOLS

c - Cohesion as defined in this paper.

$\bar{c}$ - True cohesion.

c_ϵ - Cohesion at strain ϵ.

ϵ - Axial compressive strain after consolidation.

ϕ - Angle of internal friction as defined in this paper.

$\bar{\phi}$ - True angle of internal friction.

ϕ_ϵ - Angle of internal friction at strain ϵ.

e - Void ratio.

s - Shearing strength.

S - Degree of saturation in percent.

u - Pore water pressure as measured by piezometer.

τ - Shear stress.

τ_ϕ - Shear stress on the plane of maximum stress obliquity of the frictional component of strength.

σ - Normal stress.

$\bar{\sigma}$ - Normal intergranular stress.

σ_1 - Major principal stress.

σ_3 - Minor principal stress.

$\bar{\sigma}_1$ - Major principal intergranular stress.

$\bar{\sigma}_3$ - Minor principal intergranular stress.

σ_A - Deviator stress, applied axially by the piston.

$(\bar{\sigma}_1)_c$ - Major principal intergranular stress during consolidation.

$(\bar{\sigma}_3)_c$ - Minor principal intergranular stress during consolidation.

σ_h - Triaxial cell pressure.

SECTION I

INTRODUCTION

Purpose of this investigation.

In some areas of land, great layers of silt and clay have been deposited by the process of sedimentation. As sedimentation takes place, the pressures exerted on the preceding layers become greater and greater causing the material to consolidate under the condition of no lateral yield. This type of one-dimensional consolidation in a material with static shear strength occurs with the stresses in the vertical and horizontal directions unequal; hence it is called anisotropical consolidation.

In triaxial tests the sample is usually tested by the standard method of consolidating hydrostatically and then loading until failure occurs under drained or undrained conditions. This hydrostatic stress condition prior to testing is not representative of the anisotropical stresses imposed upon the soil in its in-situ state. The purpose of this investigation is to determine what effect anisotropical consolidation has on the cohesion and friction of clay as determined by the CFS-test to be described later.

Scope of the investigation.

This paper is confined to the investigation of the effect of anisotropical consolidation on two types of remolded, near-saturated clays; commercial kaolinite and Boston blue clay. In order to compare the test results obtained from different specimens of the same clay it was necessary to use remolded samples prepared to be duplicates. A total of seventeen tests were run; four tests on Boston blue clay and thirteen tests on kaolinite. The tests were divided into five different series as follows:

Series I. Four tests were run on kaolinite subjected to varying degrees of anisotropical consolidation as determined by the consolidation stress ratio, $\left(\frac{\bar{\sigma}_1}{\bar{\sigma}_3}\right)_c$. See figure 27 of the Appendix. The major principal intergranular stress after consolidation was held as close as possible to 1.80 kg/cm^2 for all four tests. The minor principal intergranular stress after consolidation was varied to give ratios of $\left(\frac{\bar{\sigma}_1}{\bar{\sigma}_3}\right)_c$ equal to 1.00, 1.22, 1.42 and 1.59.

Series II. This series was also run on kaolinite with the major principal intergranular stress after consolidation held as close as possible to 3.65 kg/cm^2. The minor principal intergranular stress after consolidation was varied to give ratios of $\left(\frac{\bar{\sigma}_1}{\bar{\sigma}_3}\right)_c$ equal to 1.00, 1.21, 1.39 and 1.58.

Series III. In this series four tests were run on Boston blue clay. The major principal intergranular stress

after consolidation was held as close as possible to 3.65 kg/cm^2. Variations in the minor principal intergranular stress gave ratios of $\left(\frac{\bar{\sigma}_1}{\bar{\sigma}_3}\right)$ equal to 1.00, 1.20, 1.41 and 1.60.

Series IV. This series was run to determine the effect of time allowed for anisotropical consolidation. The series consisted of three tests run on kaolinite at $\left(\frac{\bar{\sigma}_1}{\bar{\sigma}_3}\right)_c$ ratios of approximately 1.60.

Series V. Two tests were run on kaolinite using different methods to consolidate the sample anisotropically. There are many methods that could be used to consolidate a sample anisotropically and three different methods were used in the whole testing program. However, the same procedure for consolidating anisotropically was used in series I, II, III and IV to avoid any effects which might be caused by using different methods.

Table 1 gives a complete summary of all tests run in this investigation.

Table 1.--Summary of test results

Series	Test No.	Sample Type	Sample No.	Test Date	$(\bar{\sigma}_1)_c$	$\left(\frac{\bar{\sigma}_1}{\bar{\sigma}_3}\right)_c$	Axial Consol. Strain cm.	Initial e	Initial S%	Final e	Final S%	Fig.
I	H-17	DWEPK	795	1-21	1.80	1.00	0.258	1.059	100.5	0.958	101.2	28
	H-18	"	793	1-24	1.83	1.22	0.378	1.057	100.9	0.948	100.2	29
	H-19	"	792	1-26	1.84	1.42	0.469	1.057	100.9	0.945	100.8	30
	H-21	"	790	2-14	1.83	1.59	0.57	1.057	100.6	0.945	100.3	31
II	H-13	DWEPK	799	12-12	3.65	1.00	0.399	1.064	99.8	0.899	99.6	32
	H-14	"	798	1-10	3.81	1.21	0.546	1.064	99.6	0.883	100.0	33
	H-15	"	797	1-13	3.69	1.39	0.686	1.053	100.6	0.887	99.7	34
	H-16	"	796	1-19	3.56	1.58	0.818	1.055	100.6	0.901	100.8	35
III	H-22	BBC	539	2-20	3.65	1.00	0.233	0.744	99.8	0.645	100.0	36
	H-23	"	538	2-23	3.66	1.20	0.35	0.758	97.6	0.651	98.2	37
	H-24	"	537	2-25	3.67	1.41	0.47	0.732	99.0	0.652	97.9	38
	H-25	"	536	3-10	3.66	1.60	0.59	0.750	98.4	0.652	98.3	39
IV	H-20	DWEPK	791	2-9	5.73	1.57	1.15	1.068	99.3	0.846	100.0	21
	H-26	"	789	3-17	3.65	1.60	1.03	1.056	100.3	0.882	100.2	22
	H-29	"	785	3-31	3.67	1.61	0.835	1.064	99.9	0.887	99.9	23
V	H-27	DWEPK	788	3-20	3.71	1.63	0.70	1.051	100.2	0.906	99.6	25
	H-28	"	787	3-24	3.64	1.60	0.96	1.060	100.1	0.895	98.9	26

SECTION II

PREVIOUS WORK DONE BY OTHERS

Anisotropical consolidation and its effect on cohesion and friction.

The writer was unable to locate previous work evaluating the effect of anisotropical consolidation on the cohesion and friction of clay. Some work has been done using anisotropical consolidation to determine the value of the at-rest earth pressure coefficient by measuring the ratio of stresses required to produce one-dimensional consolidation (1)*. Drained and undrained tests have been run on anisotropically consolidated sands and compared to hydrostatically consolidated sands by Bishop and Eldin (2). They found that for sand the most important influence of anisotropical consolidation was in the relationship between undrained strength and consolidation pressure, and that anisotropically consolidated sands had less than one-third the undrained strength of hydrostatically consolidated sands of the same composition. However, it was not clearly stated whether the strength was

*Numbers in ( ) refer to the list of references at the end of the thesis.

considered as the total difference of $(\sigma_1 - \sigma_3)$ or the further change in $(\sigma_1 - \sigma_3)$ following consolidation.

D. W. Taylor's reports, as described by Whitman, showed that for Boston clay, the ratio of the maximum shear stress at failure to the maximum principal stress after consolidation was apparently not decreased by anisotropical consolidation (3).

Measuring cohesion and friction.

The standard laboratory tests measure total strength values and do not separate cohesion and friction. The available research methods of determining cohesion and friction at failure are generally impractical because of the need of more than one sample. A complete description of these methods is given by Bjerrum in (4). Until recently no method was available to measure the variation of cohesion and friction with strain.

The well-known Coulomb-Hvorslev equation, $s = \bar{c} + \bar{\sigma} \tan \phi$, states that shearing strength is equal to the true cohesion plus the intergranular stress multiplied by the tangent of the true angle of internal friction. Hvorslev showed that, for the soils he tested, $\bar{c}$ was a function of water content only. The recent method developed by Schmertmann at the University of Florida is based on the theory that cohesion and friction can be separated by measuring the change in strength of a saturated, or near-saturated, soil due to a change in pore water pressure.

The definitions of cohesion and friction used by Schmertmann are quoted below from reference (5). They are also used in this work.

Cohesion (c).- The cohesion of a soil, at any strain, is the shear stress developed on the plane of Mohr envelope tangency at that strain, if the intergranular stress on that plane could be reduced to zero without significant change in soil structure.

Angle of Internal Friction (Ø).- The angle of internal friction, at any strain, is the angle whose tangent is the ratio of the change in shear stress to the change in normal intergranular stress occurring on the plane of Mohr envelope tangency at that strain, during a stress change occurring without significant change in soil structure.

SECTION III

EQUIPMENT USED AND TESTING PROCEDURE

Equipment used.

The triaxial equipment used was that developed by the Norwegian Geotechnical Institute and purchased from Geonor A/S, Forskningsveien 1, Oslo-Blindern, Norway. The only modification was in the triaxial units where the standard bushing and piston were replaced by Harvard ball-bearing pistons. The device used for anisotropical loading was also manufactured by Geonor A/S. Figure 1 shows the triaxial cell with the anisotropical loading mechanism during a test. Complete description of the equipment can be found in (6).

The testing machine is designed such that the triaxial cell rests on a table that moves upward at a constant rate against a proving ring. Thus the strain rate of the sample depends upon the rate of change in load on the proving ring. If the load on the sample is nearly constant, as in the latter part of the test, then all of the table movement is used to strain the sample, but if the load is increasing rapidly as in the beginning of the test, then most of the table movement is used to compress the proving ring. The above phenomenon results in a test run at a varying rate of strain.

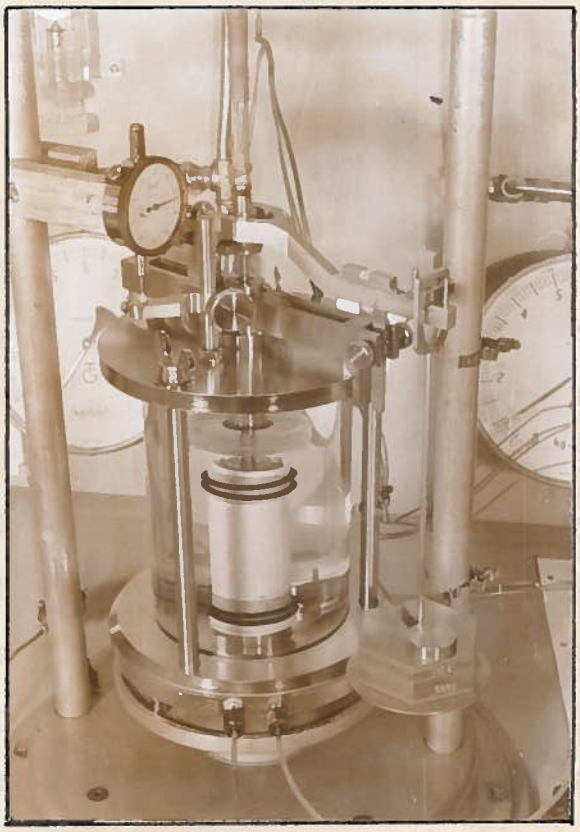

Fig. 1.--Triaxial cell with anisotropical loading mechanism.

In order to eliminate the variable rate of strain in the tests, a more rigid type of device for measuring the load on the piston was developed by the author to be used in place of the proving ring. This was made from a section of aluminum tubing, six inches long, 3/8" O. D. with a wall thickness of 0.027 inches. A two inch section in the center was turned down so that the wall thickness was only about 0.002 inches thick. Mounted on this thin-walled section are four SR-4, type C-7 electrical strain gages. Two gages were mounted longitudinally on each side of the tube and connected in series to compensate for eccentric loads on the tube. The gage and wiring diagram are shown in figure 2. Since the type C-7 gages are sensitive to temperature changes (a beam of light from a flashlight two feet away will change the reading), the compensating gages were mounted on the same tube in a transverse direction. This reduces fluctuations from temperature changes to a minimum and also increases the sensitivity due to the Poisson effect.

After the gages were mounted and the electrical connections soldered, the tube was dipped into molten wax to seal the gages from any changes in humidity which might cause fluctuations in the readings. Two layers of wool yarn were also wound around the gages as an insulator. The testing laboratory is air conditioned and the temperature variations are never over one or two degrees

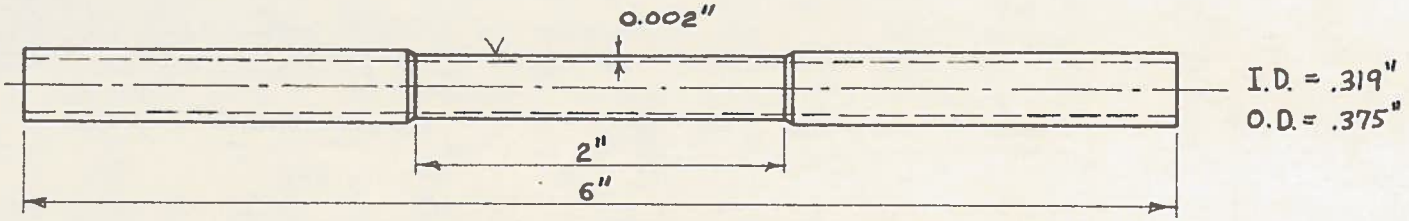

High Strength Aluminum Tubing

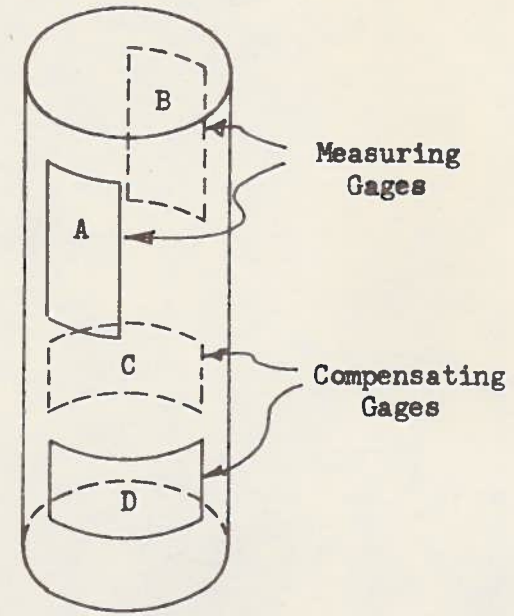

Gage Orientation

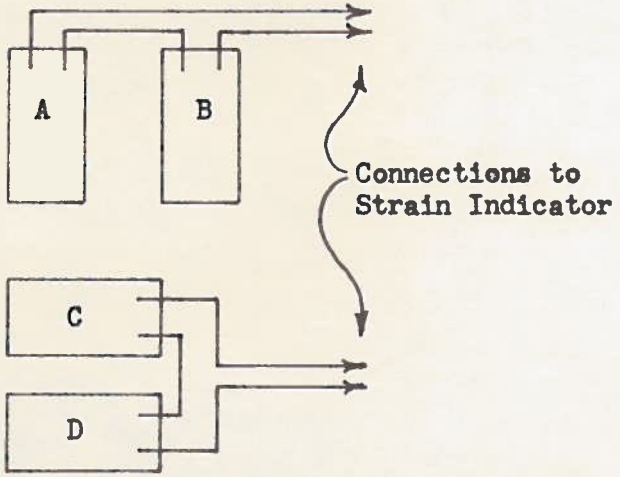

Wiring Diagram

Fig. 2.--Load cell and wiring diagram

Fahrenheit. Thus, the effects from temperature variations were virtually eliminated.

The rigidity of the load cell was on the order of eighteen times greater than the proving ring of the same load range. The sensitivity is such that the gage factor of the strain indicator could be adjusted to give a calibration of 100 grams per 10 micro inches per inch. The load cell gives a linear load calibration curve which the proving rings did not have, thus eliminating the need for reference to a calibration curve. The gages have given very satisfactory service and give stable readings over considerable lengths of time. The tests usually ran thirteen to twenty-four hours. The load cell described above had a capacity of forty kg. Larger cells were made to accommodate greater loads. However, the sensitivity decreases as the capacity is increased.

In order to meet the requirements of duplicate samples with a high degree of saturation, a "Vac-Aire" extruder was used which is capable of producing round bars of clay with almost 100 percent saturation (7). After the samples were extruded and cut to the desired length, they were sealed in wax until tested. Good results were obtained using this method.

Sample preparation.

Kaolinite. The kaolinite samples were prepared from kaolinite which was obtained from the Edgar Plastic Kaolin

Company, in Edgar, Florida. This is a relatively pure commercial kaolinite. It was mixed with distilled water to give a water content between 40% and 41%. These samples were designated as DWEPK. The clay was thoroughly mixed by hand and passed through the extruder several times to insure samples of uniform structure and water content.

Boston blue clay. The Boston blue clay was obtained from a pit in Cambridge, Massachusetts, by Professor Schmertmann, who prepared the samples and permitted their use in this research. Upon remolding, the clay had to be allowed to partially dry in order to gain sufficient strength for extrusion into round bars. It was finally extruded at a water content of 26%. These samples contained only their natural water since no water was added to them. They were cut and dipped into wax just as was done for the kaolinite. These samples were designated as BBC.

Table 2 lists the Atterberg limits, specific gravity and grain size analysis of both clays.

Table 2.--Clay Properties

Clay	L.L. %	P.I. %	G	Percent finer than		
				200 Sieve	50μ	2μ
DWEPK	52	21	2.61	100	100	70
BBC	38	19	2.81	97.9	87.0	52.5

After the samples were extruded from the "Vac-Aire" extruder, they were stored for a sufficient length of time to allow for any thixotropic action to take place, as determined by laboratory vane shear tests. When ready for use, the sample was carefully stripped of its wax covering and placed in a 10 cm. miter box. Each end of the sample was then marked by use of a template for the position of the internal drains, the holes for which were then punched through the sample with a long sewing needle mounted in a drill press. The number of drains to be used was governed by the permeability of the clay to be tested. In the kaolinite samples only one drain was used while in the Boston blue clay three drains were used. Saturated wool yarn was threaded through the punched holes and the sample was then placed in a miter box where it was trimmed to the 8.0 cm. length used for testing. The sample diameter used was the extruded diameter of 3.58 cm.

After the sample was prepared for testing it was placed in the triaxial cell with filter strips along the sides and filter discs on the top and bottom of the sample. A porous stone was placed at the bottom where the connections for drainage and pore pressure control were located. Two "Shiek" brand prophylactics were used with a layer of type M, Apiezon grease between them to seal the sample from the cell pressure media (water). The grease was used as an extra precaution against migration of water into the

sample since the tests were run at relatively high pressures and over long periods of time.

Testing procedures.

Anisotropical consolidation. In order to study the effect of anisotropical consolidation as compared to hydrostatic consolidation, the tests were run such that the only variable was the minor principal intergranular stress during consolidation. The major principal intergranular stress was held nearly constant for each series giving consolidation stress ratios, $\left(\frac{\bar{\sigma}_1}{\bar{\sigma}_3}\right)_c$, of 1.0, 1.2, 1.4, and 1.6. The "consolidation stress" as used herein is the maximum principal intergranular stress during consolidation.

The method used for consolidating the samples for series I, II, III and IV is as follows: With the anisotropical loading device developed by Geonor A/S, the weights are suspended on a hanger which transmits the load to the piston of the triaxial cell through a system of knife edge supports at a lever arm ratio of 5. The load to the piston is five times the load applied to the hanger. After noting the characteristic shape of the consolidation curves for kaolinite under a hydrostatic pressure of 3.65 kg/cm^2, it was observed that at approximately 6 ml. decrease of volume, as measured by the amount of water drained from the sample into a burette, the consolidation curve starts into secondary consolidation. The total volume change was slightly over 7 ml. It was decided to add the weights at

equal intervals of volume change such that all of the weights would be added by the end of 6 ml. or 6/7 of the total consolidation. The weight increments used were determined by the convenience of the size of weights available. This load increment was usually 1 kg. on the sample and a range of four to eleven increments were used. The cell pressure was applied in one step at the beginning of consolidation and remained constant throughout the above piston loading cycle.

The reason for not adding all of the anisotropical load at the beginning of consolidation is that the sample is not able to support the total load without excessive strain or possible failure. By adding the load after equal increments of volume change, the sample is given time to build up strength to support the following load increment without excessive strain.

In series V, two methods of consolidation were used. For test H-27 the sample was first consolidated hydrostatically under a pressure of 2.28 kg/cm^2. After the consolidation had proceeded 1370 minutes into the secondary stage, the axial load was then applied in eleven increments, with 4.55 minutes between increments, until the maximum principal intergranular stress, $(\bar{\sigma}_1)_c$, was equal to 3.71 kg/cm^2. The sample for test H-28 was consolidated in a different manner. The axial load and cell pressure were both increased in six increments allowing the sample to consolidate for eight hours between each increment.

The sample was subjected to a consolidation stress ratio of 1.6 at all times during the consolidation. The final stress values on the sample were, $\bar{\sigma}_3 = 2.28$ kg/cm^2 and $\bar{\sigma}_1 = 3.64$ kg/cm^2.

It was thought that the above variations of consolidating the clays anisotropically would exhibit any effects that would be caused by the method used to arrive at the final stress condition.

Strength testing. The testing procedure used for all tests was the CFS-test which was developed by Professor John H. Schmertmann at the University of Florida. A detailed procedure for the performance of this test may be found in (5).

The anisotropical loading device is designed such that the CFS-test can be started without having to remove the deviator stress which was applied for anisotropical consolidation. Thus, the total load on the sample during testing was the sum of that applied by the load cell and that applied by the anisotropical loading device.

The compression rate was chosen to be the same for all tests and was equal to 0.005 mm./min. This strain rate was such that the required data for computing cohesion and friction over the range of approximately ½ to 5% strain could be obtained over a compression period of about twelve hours.

SECTION IV

COMPUTATION OF RESULTS

Data corrections.

A general outline of how measurements were taken will now be explained. A schematic diagram of the triaxial apparatus is shown in figure 3. Volume changes are measured by the use of mercury manometer 'b' connected between the triaxial cell and the pressure cell. Pore pressure is controlled by mercury manometer 'a' acting in series with the back pressure exerted by hydraulic load cell 'A'. Any change in the volume of the sample is reflected by a change in the manometer reading, Δb, which also results in a small change of cell pressure. The magnitude of Δb is kept within $\pm$ 0.05 kg/cm^2 by adjusting the screw control 'II' between the triaxial cell and the manometer. Volume changes are computed on the basis of the inside diameter of the plastic tubing used in the mercury manometers.

Several corrections were made to the data after running the tests. The volume change reading is corrected for oil seepage past the piston and also for the volume of the piston entering the triaxial cell. A correction is also made to the cell pressure corresponding to the reading Δb. The amount of volume change is converted to sample

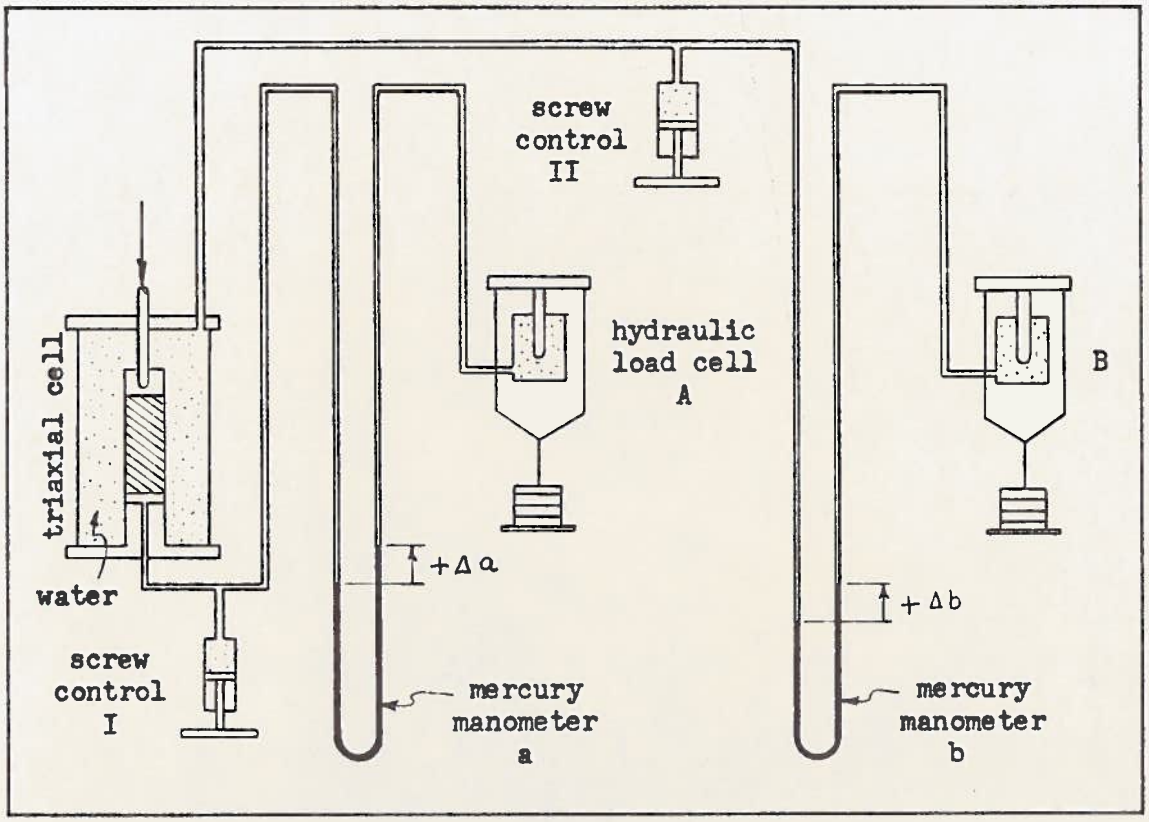

Fig. 3.--Schematic diagram of triaxial apparatus during CFS-test after Schmertmann and Osterberg (5)

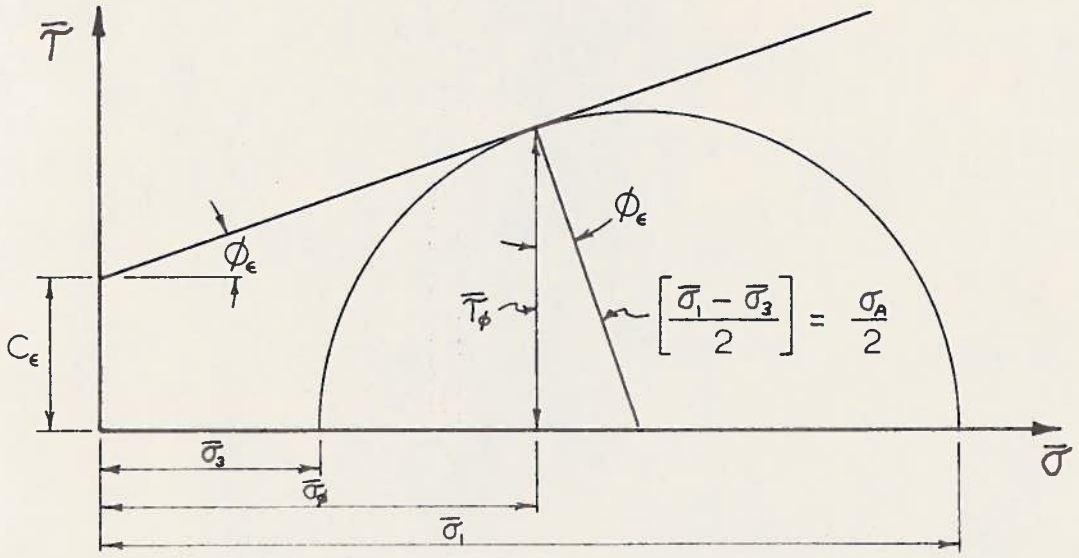

Fig. 4.--Mohr's circle of stress at strain, ϵ, after Schmertmann and Osterberg (5)

strain from measurements taken of axial strain vs. volume change when the sample is consolidated hydrostatically. Sample strain is measured with a dial indicator that records the movement of the table during the test. This reading is corrected for strain in the load cell, which amounts to 0.005 mm. per kg. of load. There is also a correction for the change in intergranular stress, which causes an expansion or contraction of the mechanical system of the triaxial cell, due to pore pressure changes.

The sample area is corrected for strain on the assumption that the specimen remains as a right circular cylinder during compression according to the formula $A' = A/(1 - \epsilon)$ where A' is the area at a given strain, ϵ, and A is the area of the sample at zero strain.

Calculation of cohesion and friction from the stress-strain curves.

Stress-strain curves are computed from the corrected data and plotted showing the computed values of intergranular stress for each point. A smooth curve is drawn through the high and low intergranular stress curves and the values of axial stress along with the corresponding values of intergranular stress are scaled off at a given strain. These values are then used to compute the value of cohesion and friction in the sample at that strain. Schmertmann showed that at any given strain, ϵ, the strength of the sample is governed by the Coulomb-Hvorslev

equation,

$$\bar{\tau}_\phi = C_\epsilon + \bar{\sigma}_\phi \tan \phi_\epsilon . \qquad (1)$$

In the triaxial test,

$$\bar{\sigma}_1 = \sigma_A + \sigma_3 - u$$

and

$$\bar{\sigma}_3 = \sigma_3 - u .$$

Therefore,

$$\bar{\sigma}_1 - \bar{\sigma}_3 = \sigma_A .$$

From figure 4, $\bar{\tau}_\phi = \frac{\sigma_A}{2} \cos \phi_\epsilon$

and $\bar{\sigma}_\phi = \bar{\sigma}_3 + \frac{\sigma_A}{2} - \frac{\sigma_A}{2} \sin \phi_\epsilon .$

Inserting the expressions for $\bar{\tau}_\phi$ and $\bar{\sigma}_\phi$ into (1) gives, upon simplification,

$$\frac{\sigma_A}{2} = \left(\frac{\sin \phi_\epsilon}{1 - \sin \phi_\epsilon}\right) \bar{\sigma}_3 + C_\epsilon \left(\frac{\cos \phi_\epsilon}{1 - \sin \phi_\epsilon}\right). \qquad (2)$$

This is the equation of a straight line where $\sigma_A = f(\bar{\sigma}_3)$ for any constant value of strain. Thus at any fixed value of strain two points on this line can be determined from the stress-strain curves of the CFS-test. By letting $\frac{\sigma_A}{2}$ be the dependent variable, the slope of the line is equal to $\frac{\sin \phi_\epsilon}{1 - \sin \phi_\epsilon} = \frac{\Delta\left(\frac{\sigma_A}{2}\right)}{\Delta \bar{\sigma}_3}$ from which the angle of internal friction and the intercept of the ordinate can be computed which is equal to $C_\epsilon \left(\frac{\cos \phi_\epsilon}{1 - \sin \phi_\epsilon}\right)$. Hence, the cohesion and friction can be computed at any value of strain from the relationship between the axial deviator stress and the minor intergranular stress.

SECTION V

PRESENTATION AND ANALYSIS OF TEST RESULTS

Consolidation characteristics.

Series I, II and III. The method used for consolidating these series has been previously explained on pages 15 and 16. Figures 5, 6 and 7 show consolidation plotted as axial compression while figures 8, 9 and 10 show consolidation plotted as volume change. Volume changes were determined by measuring the amount of water squeezed out of the sample during consolidation into a burette attached to a connection leading to the porous stone at the base of the sample.

One distinguishing feature of these curves is that the amount of volume change is a function of the major principal intergranular stress only and is independent of the minor principal intergranular stress. This phenomenon was observed by Rutledge in (8). He stated that the relation between the major principal intergranular stress and water content was independent of the minor and intermediate principal stresses for saturated clays. The tests presented in this paper agree with his observations.

The amount of axial strain that takes place during consolidation, however, varies almost directly with the

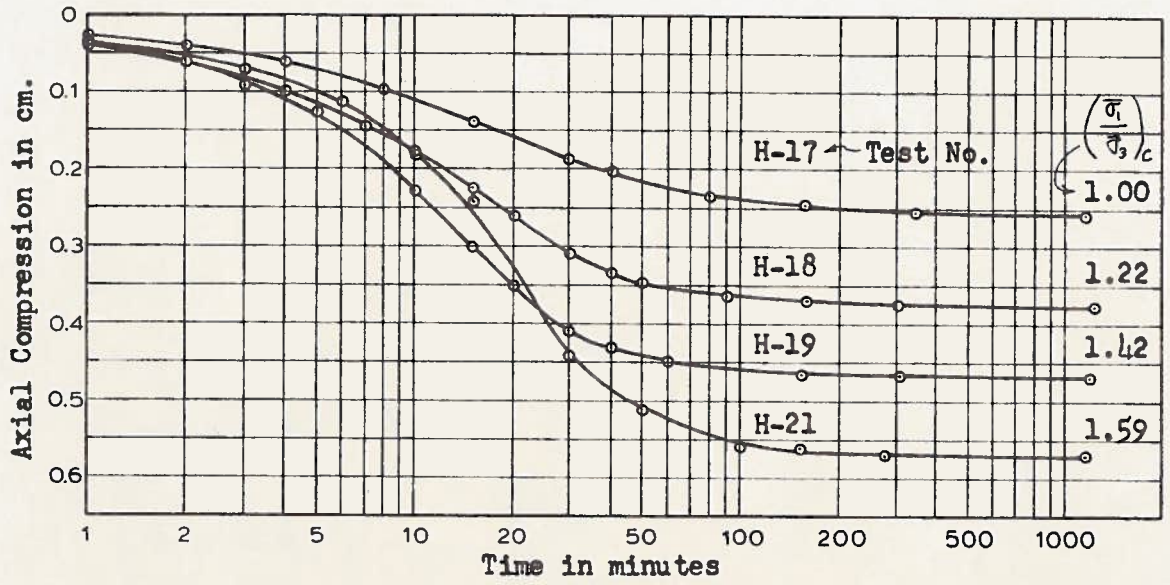

Fig. 5.--Consolidation curves for series I (kaolinite)

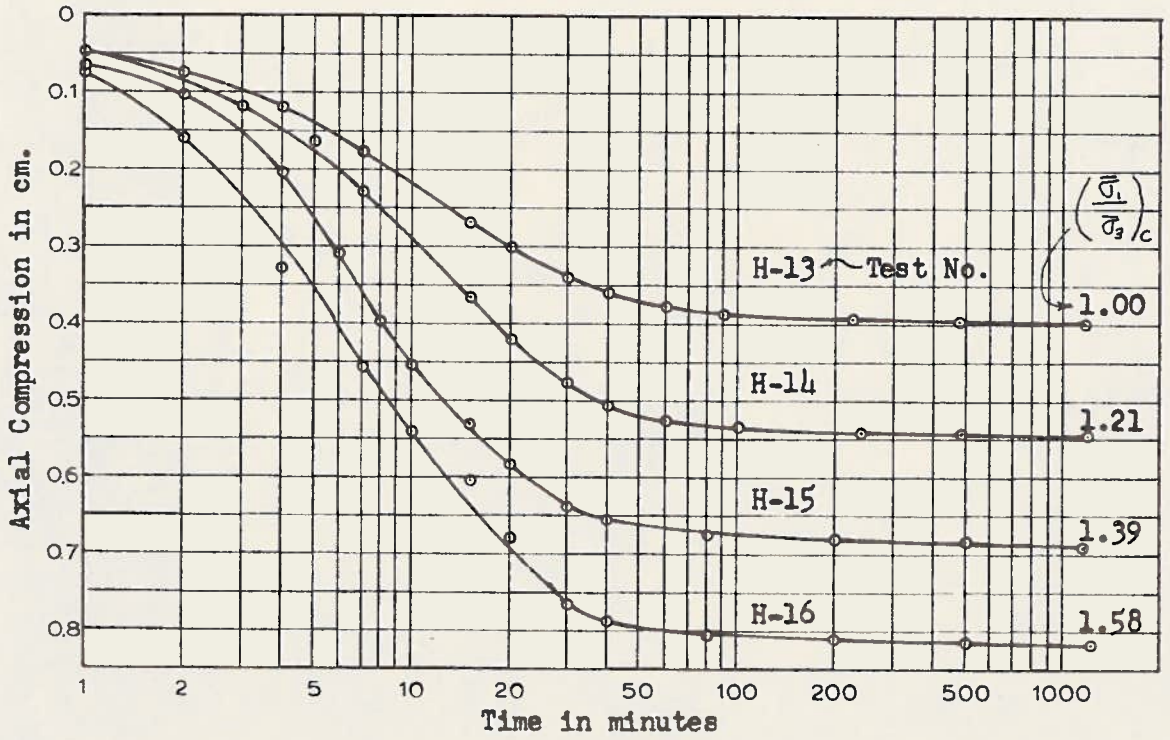

Fig. 6.--Consolidation curves for series II (kaolinite)

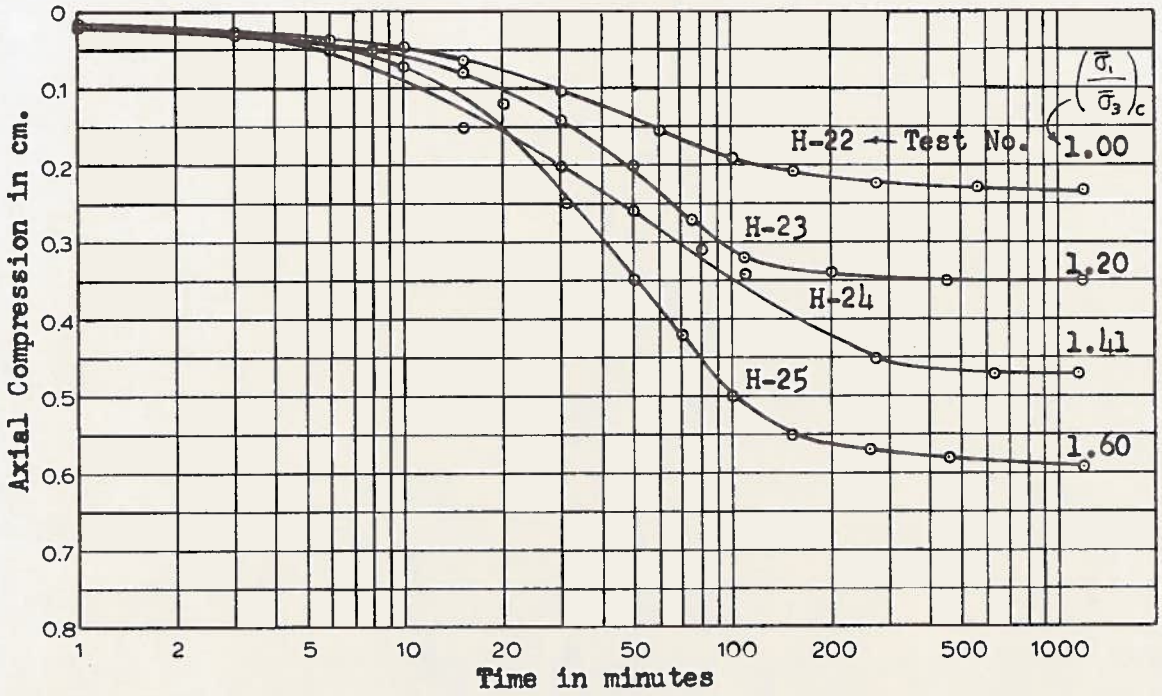

Fig. 7.--Consolidation curves for series III (Boston blue clay)

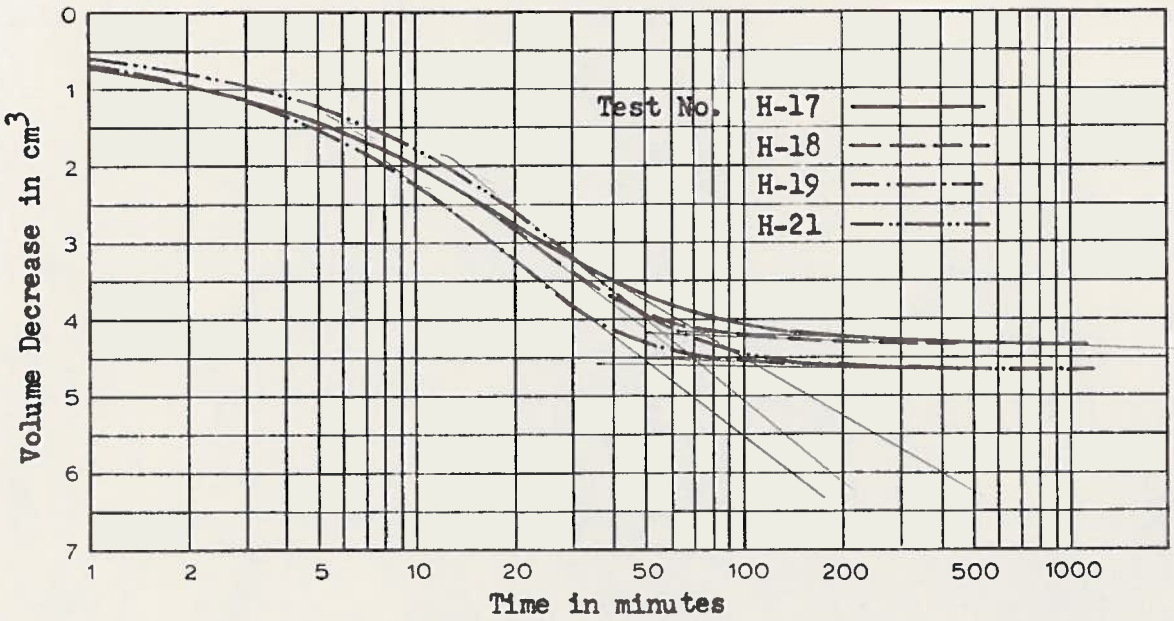

Fig. 8.--Consolidation curves for series I (kaolinite)

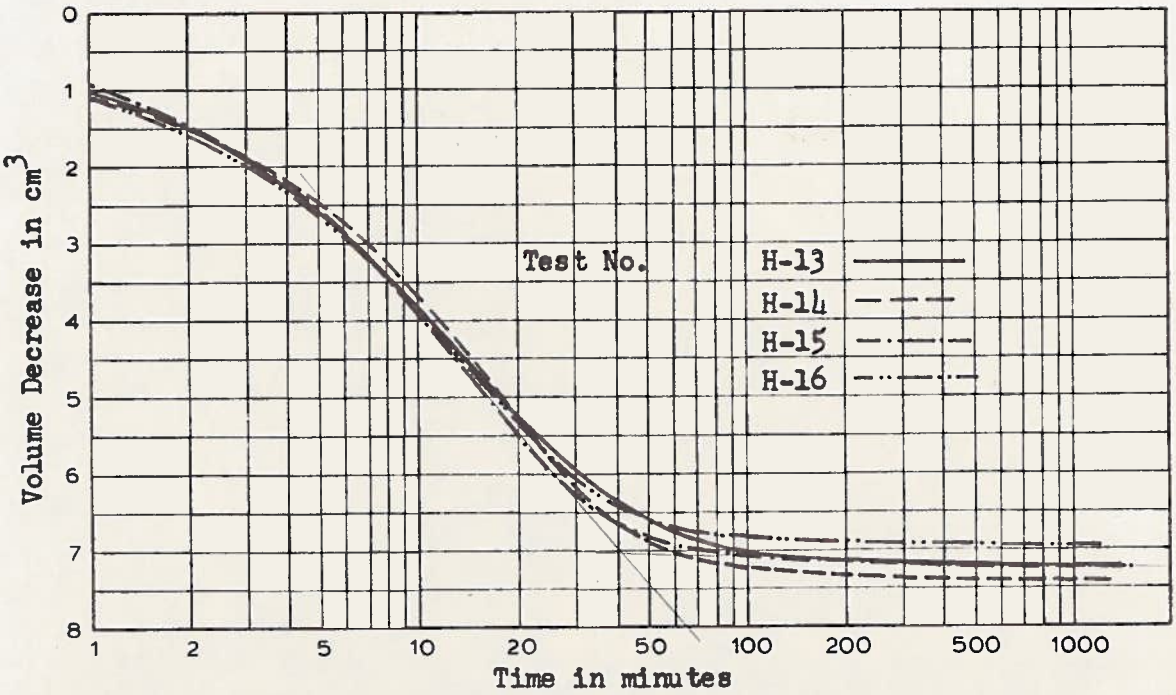

Fig. 9.--Consolidation curves for series II (kaolinite)

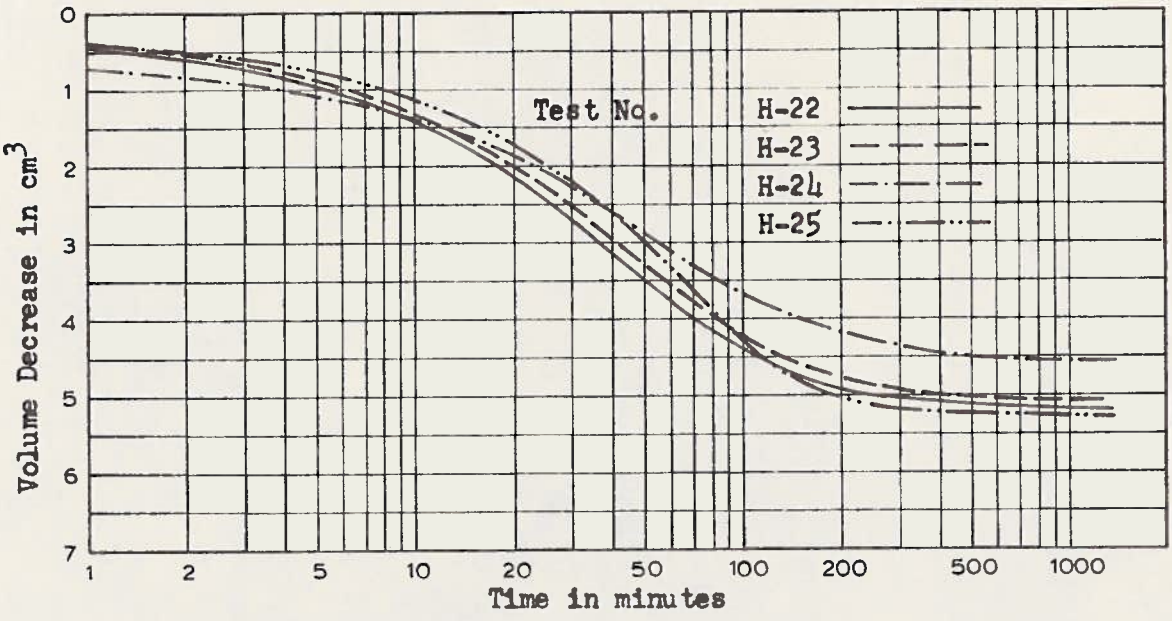

Fig. 10.--Consolidation curves for series III (Boston blue clay)

consolidation stress ratio. This is what would be expected since the deviator stress acting during consolidation increases with increasing values of $\left(\frac{\bar{\sigma}_1}{\bar{\sigma}_3}\right)_c$ used.

If the change in average cross-sectional area before and after consolidation is computed and this value is expressed as a percent, curves as shown in figures 11, 12 and 13 are obtained when the change in area is plotted against consolidation stress ratio $\left(\frac{\bar{\sigma}_1}{\bar{\sigma}_3}\right)_c$. The point at which the change in area is zero gives the ratio of stresses required for one-dimensional consolidation. A value of the at-rest earth pressure coefficient can thus be obtained. For kaolinite the values obtained were 0.68 for a maximum principal intergranular stress of about 1.83 kg/cm^2, and 0.70 for a maximum principal intergranular stress of about 3.65 kg/cm^2. Boston blue clay gave a value of 0.63 for a maximum principal intergranular stress of 3.66 kg/cm^2. However, since the change in area depends upon how the sample is anisotropically consolidated, the values given above are not necessarily correct.

A much better method for determining the at-rest earth pressure coefficient for a given soil is given by Bishop in (1). The method described is as follows: By slowly increasing the cell pressure and at the same time observing the volume change that takes place, the sample is strained the amount that it would have if all of the strain were in the axial direction. The stresses required

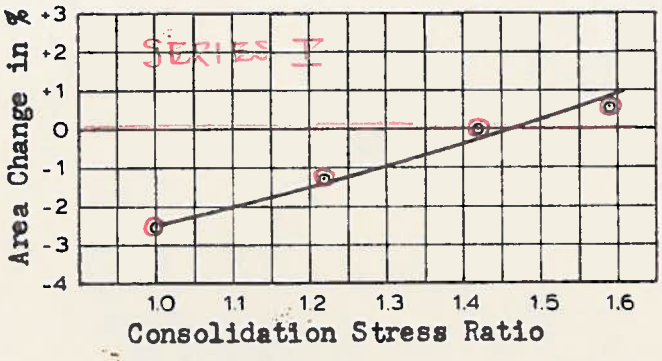

Fig. 11.--Area change vs. consolidation stress ratio for series I (kaolinite)

Change in ave. x-sectional area of specimen during consolidation

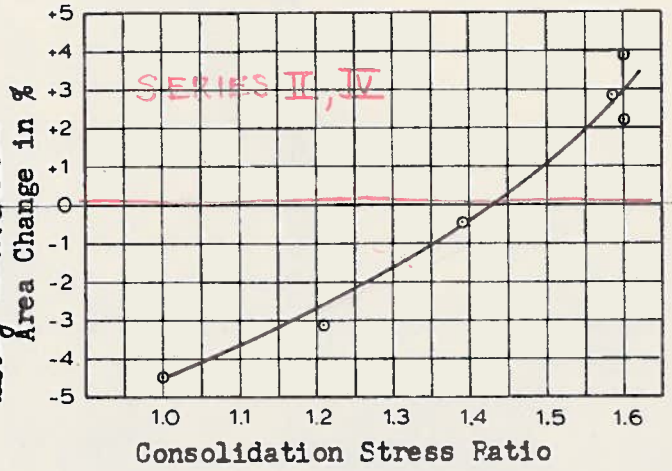

Fig. 12.--Area change vs. consolidation stress ratio for series II (kaolinite) and IV

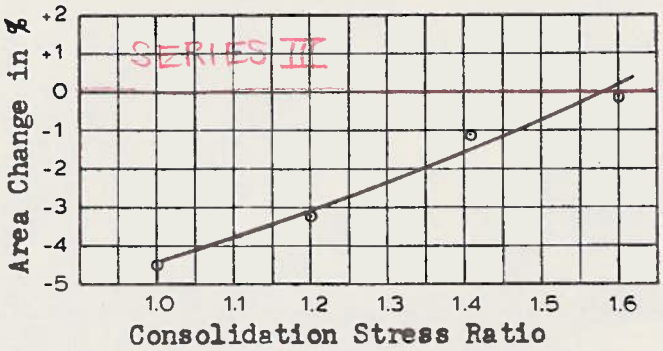

Fig. 13.--Area change vs. consolidation stress ratio for series III (Boston clay)

to maintain this condition give the relationship necessary to compute the at-rest earth pressure coefficient.

Another point to mention is the fact that secondary consolidation is practically non-existent and was apparently not affected by the consolidation stress ratio. The phenomena of consolidation is not considered in detail in this paper, but it is noteworthy to mention the large discrepancy between the consolidation curves obtained in the triaxial cell and those obtained in the standard consolidation ring as found by MacFarlane (9). His tests on kaolinite show appreciable slopes in the secondary consolidation range while the ones presented in this paper show much smaller slopes in all cases.

Series IV. The consolidation curves for the tests in series IV are merely duplicates of those in series II and are not included since the main purpose of running the tests was to analyze the time effects on cohesion and friction. The same consolidation procedure as in series I, II and III was used in these tests.

Series V. It was observed in test H-27, figure 14, that additional consolidation due to the addition of increments of axial load did not commence until a certain stress was reached. The $(\sigma_1 - \sigma_3)$ stress required to start consolidation was between 0.68 and0.80 kg/cm^2 as shown in the figure assuming the area of the sample to be 10 cm^2. This would fall near the value of twice the peak cohesion for the sample if it were consolidated hydrostatically

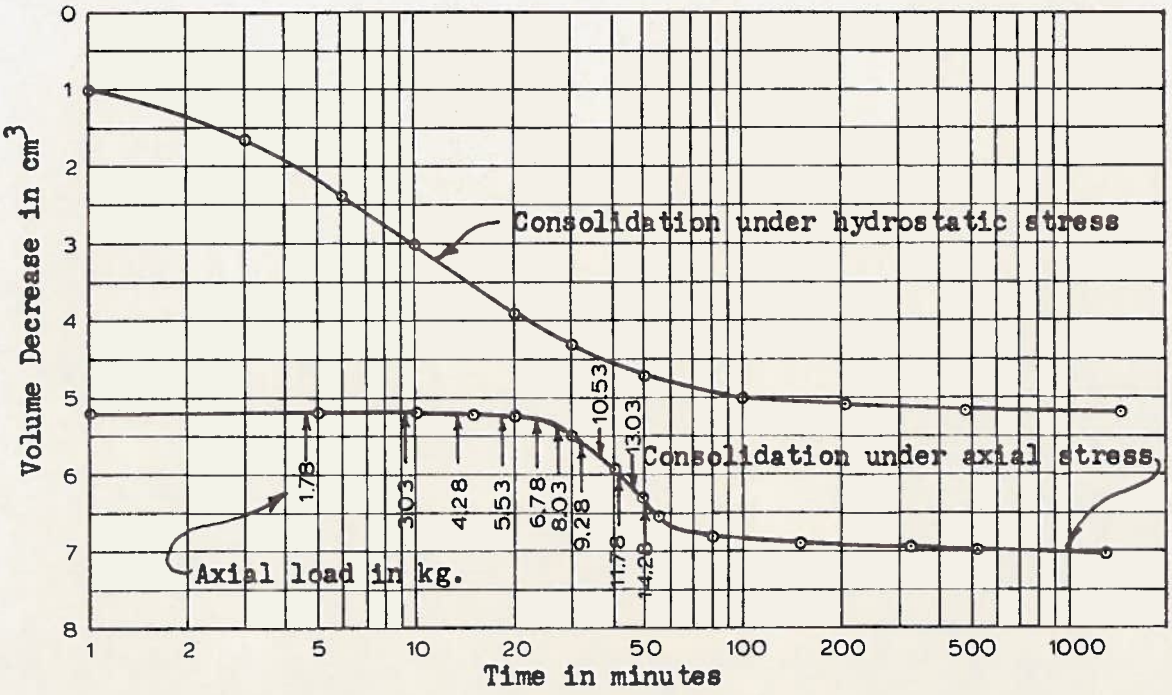

Fig. 14.--Consolidation curves for test H-27

to a pressure of 2.28 kg/cm^2. Terzaghi observed similar behavior in a paper given at the 4th Texas Conference (10). He described the consolidation of undisturbed layers of clay as a process of breaking down the solid water layer between the clay particles and placing them into a lubricated condition. Consolidation in a normal fashion will not take place until a stress is reached that is capable of breaking down this solid water layer. Further tests would be required to draw any definite conclusions.

Tests H-27 and H-28, table I, show the difference in the amount of strain during consolidation that can be caused by using different methods of consolidating anisotropically. Test H-27 strained 0.70 cm. as compared to 0.96 cm. in test H-28. The comparable test in series II, (H-16), strained 0.818 cm. during consolidation.

Cohesion and friction.

Figures 15 through 20 show composite curves of cohesion and friction plotted against strain for series I, II and III. Individual curves are shown for every test and can be found from the list of figures in table I.

Under anisotropical consolidation the sample is initially supporting a deviator stress, σ_A , and it is represented by a small circle on the vertical axis of the stress-strain curves of each test. In order to support this deviator stress, the initial values of cohesion and friction cannot both be zero. If the sample is subjected

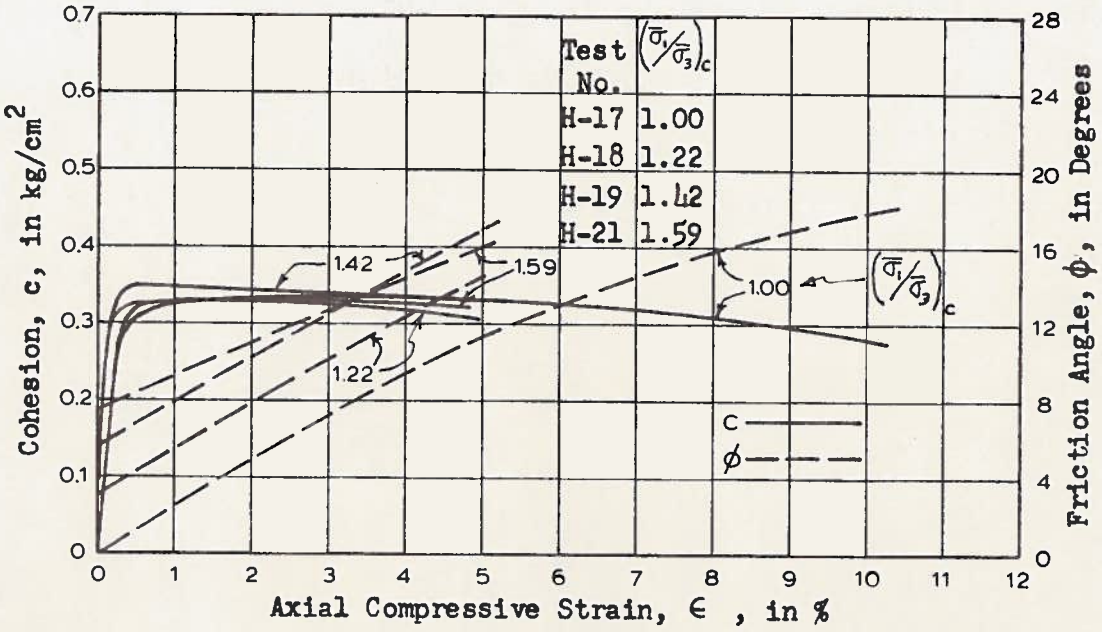

Fig. 15.--Variation of cohesion and friction with strain for series I

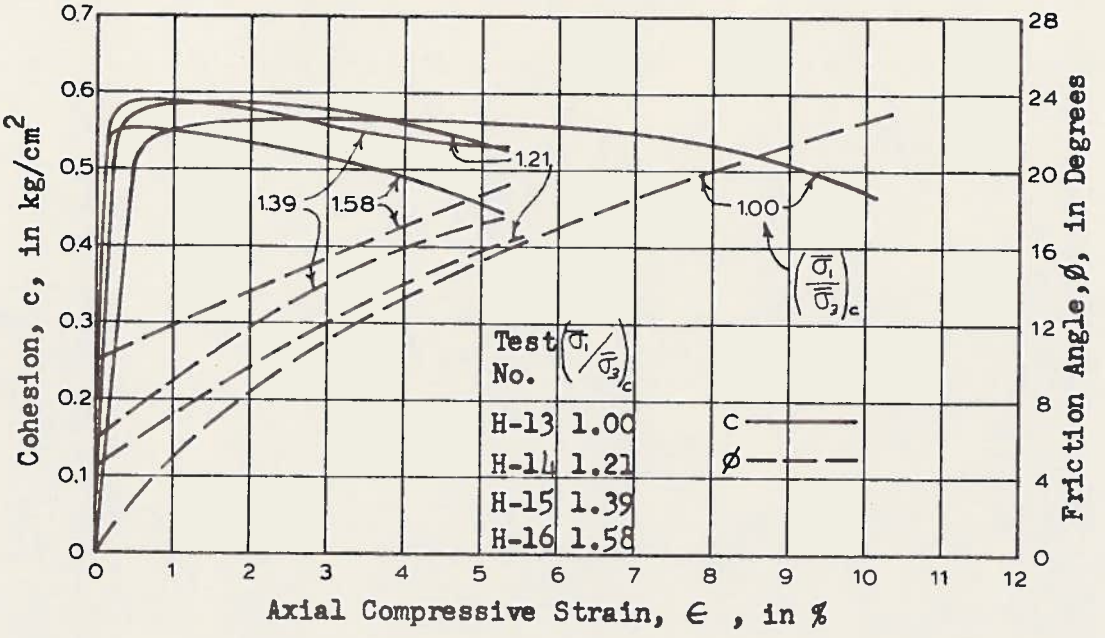

Fig. 16.--Variation of cohesion and friction with strain for series II

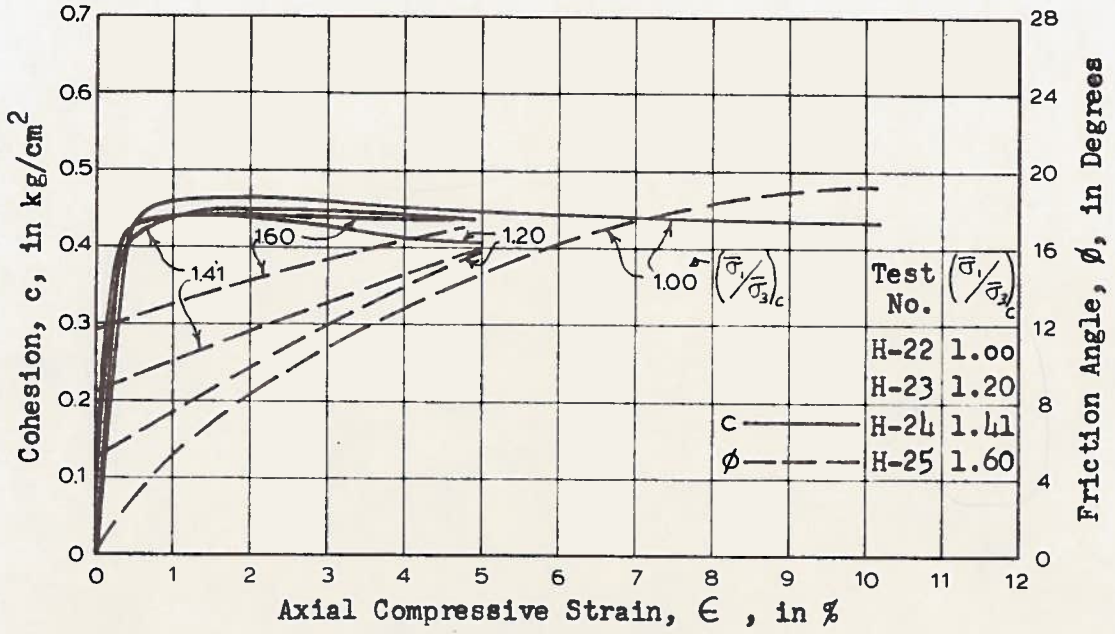

Fig. 17.--Variation of cohesion and friction with strain for series III

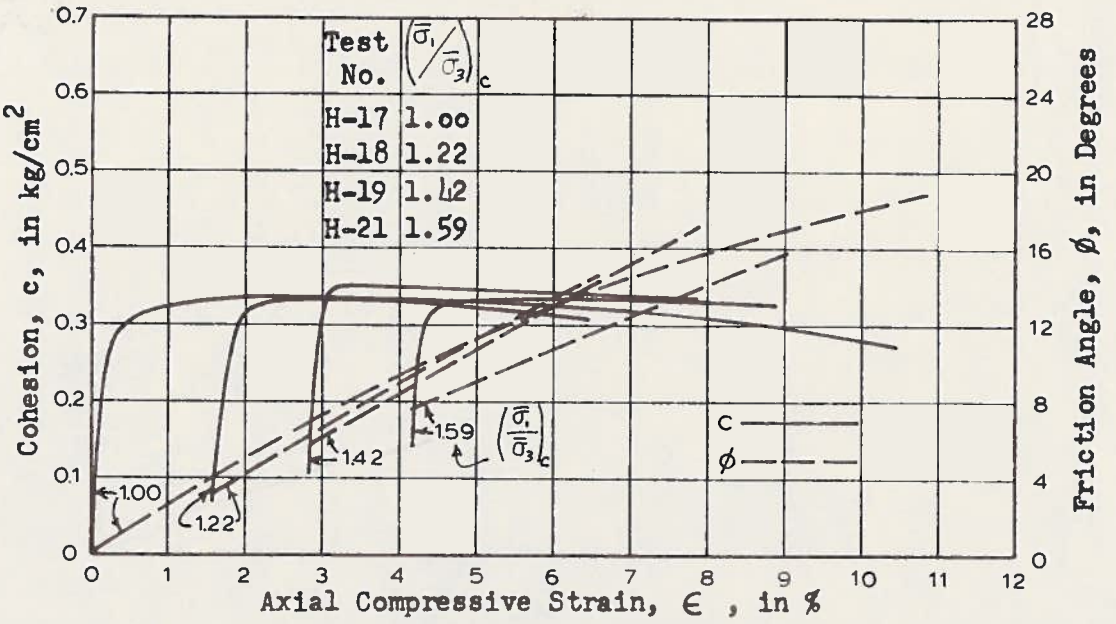

Fig. 18.--Variation of cohesion and friction with strain for series I

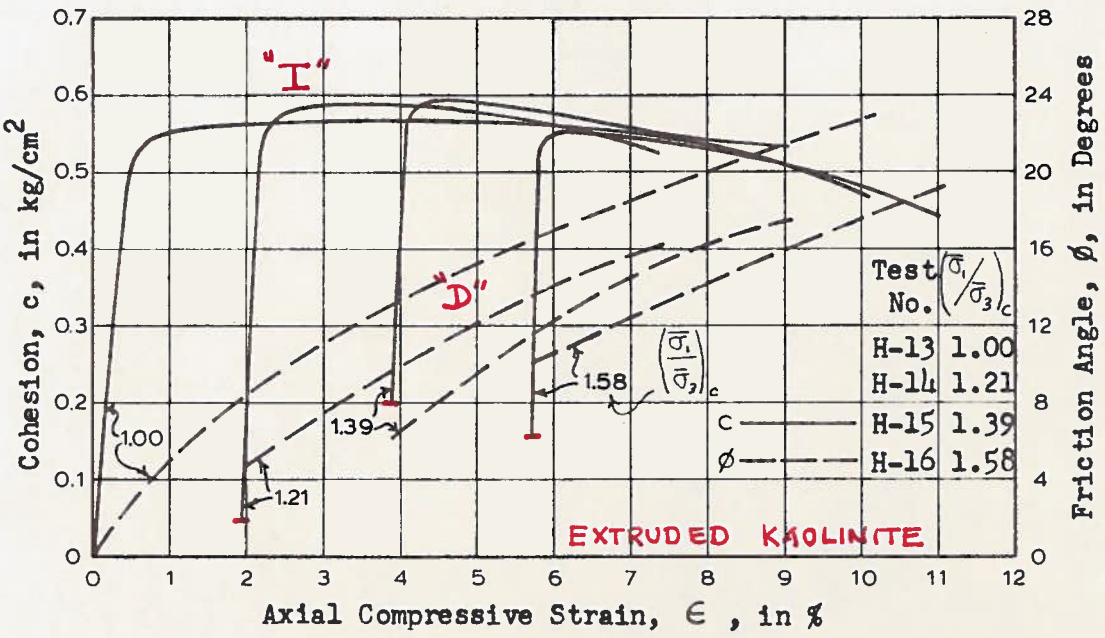

Fig. 19.--Variation of cohesion and friction with strain for series II

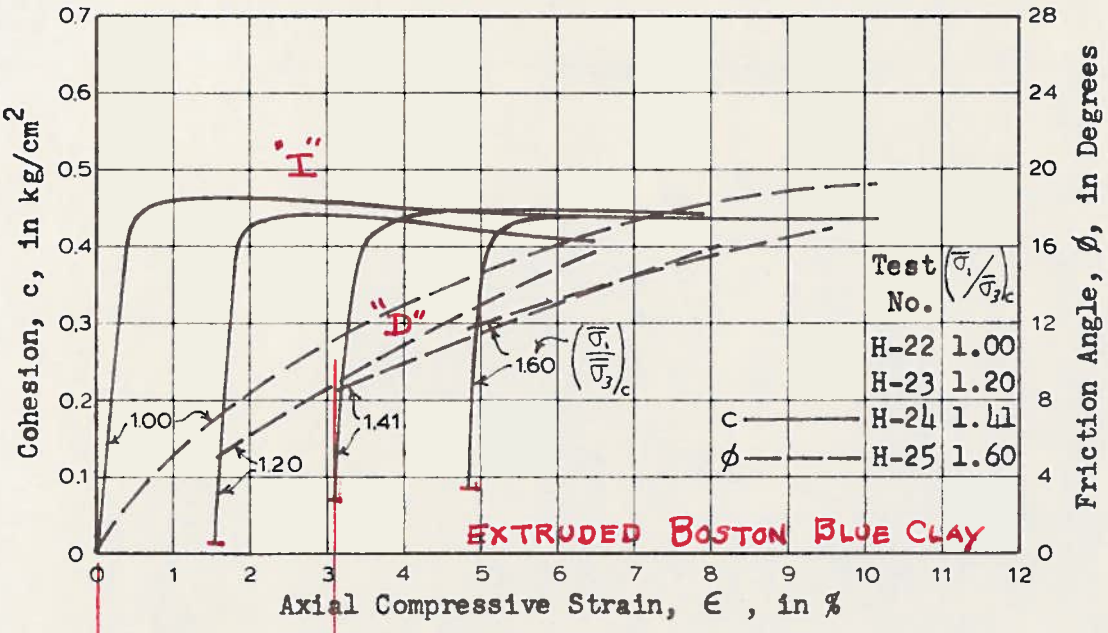

Fig. 20.--Variation of cohesion and friction with strain for series III

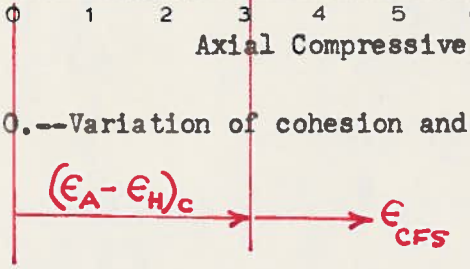

to a hydrostatic state of stress as in the case of hydrostatic consolidation, then at zero strain both the cohesion and friction are assumed to be zero. For the anisotropical case the following method was used to compute the values of cohesion and friction at zero strain. The values of cohesion and friction were computed only at strains where the two required $\bar{\sigma}_1$ curves are fully defined and they are plotted against that strain. Since it is impossible, from the data obtained, to draw the two curves for different intergranular stresses at very small values of strain (less than 0.25%), an extrapolation procedure was used. The frictional component of strength is believed to vary less rapidly with strain than the cohesion, and thus the friction was extrapolated to zero strain instead of the cohesion. This value of friction is assumed to be the value at zero strain and is used to compute the value of cohesion at zero strain by substituting into equation 2. The initial values of cohesion and friction as computed by this method are shown on the curves plotted for the individual tests as well as the curves showing each complete series.

Series I, II and III. These three series have the same characteristics for cohesion and friction and will therefore be discussed together. In figures 15, 16 and 17 it can be seen that cohesion is a function of the maximum principal stress. The frictional component acts as if

the hydrostatic friction curve were progressively displaced upward for increasing values of $\left(\frac{\bar{\sigma}_1}{\bar{\sigma}_3}\right)_c$.

During anisotropical consolidation the samples undergo an additional axial strain over that which they would under hydrostatic consolidation. It might be thought that this additional strain causes the development of friction in a relationship given by the development rate of friction for the hydrostatically consolidated sample when it is strained. However, this is not the case as shown in figures 18, 19 and 20. These figures have been plotted by displacing the computed results by that amount of strain which is in excess of that caused if the sample were consolidated hydrostatically. In every case the values for the friction fall below that which would be predicted from the hydrostatically consolidated sample.

Series IV. Three tests were run to determine the effect of the length of time permitted for anisotropical consolidation on CFS-test behavior. These test results are shown in figures 21, 22 and 23. The three tests show no marked differences in their results. When the value of friction was extrapolated to zero strain to compute cohesion at zero strain, the computed value of cohesion ranged from -.08 to 0 kg/cm^2. The value of cohesion was then assumed to be zero and the value of friction extrapolated to zero strain was adjusted to suit this condition.

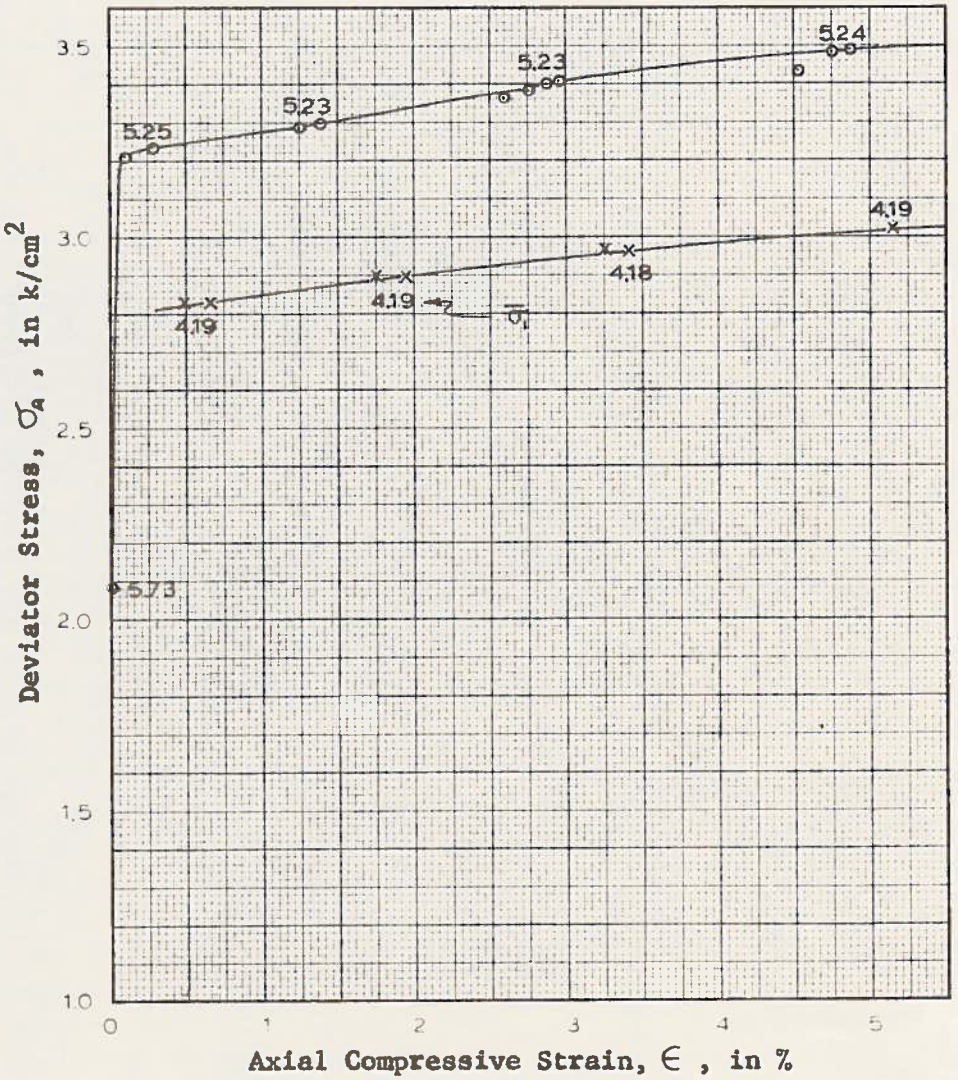

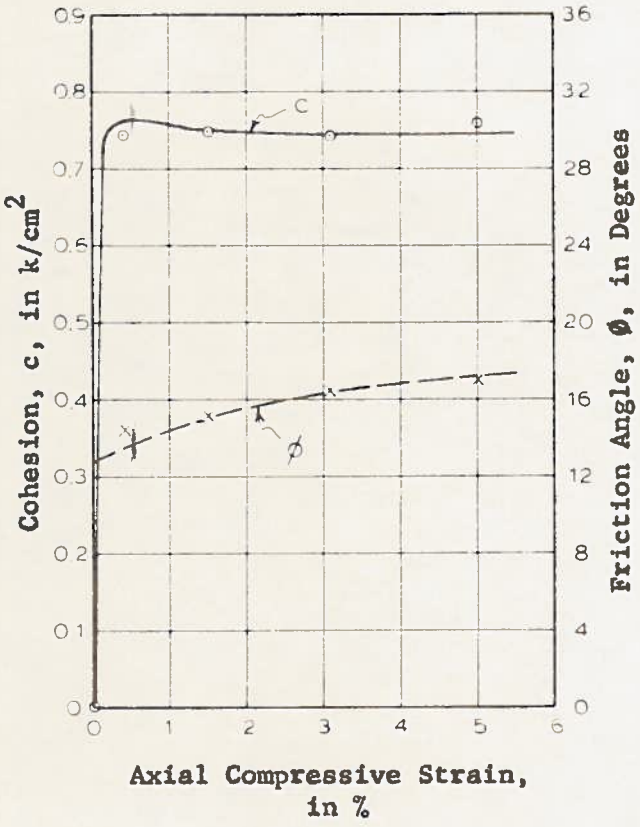

Fig. 21.--Stress-strain curves and computed results for test H-20

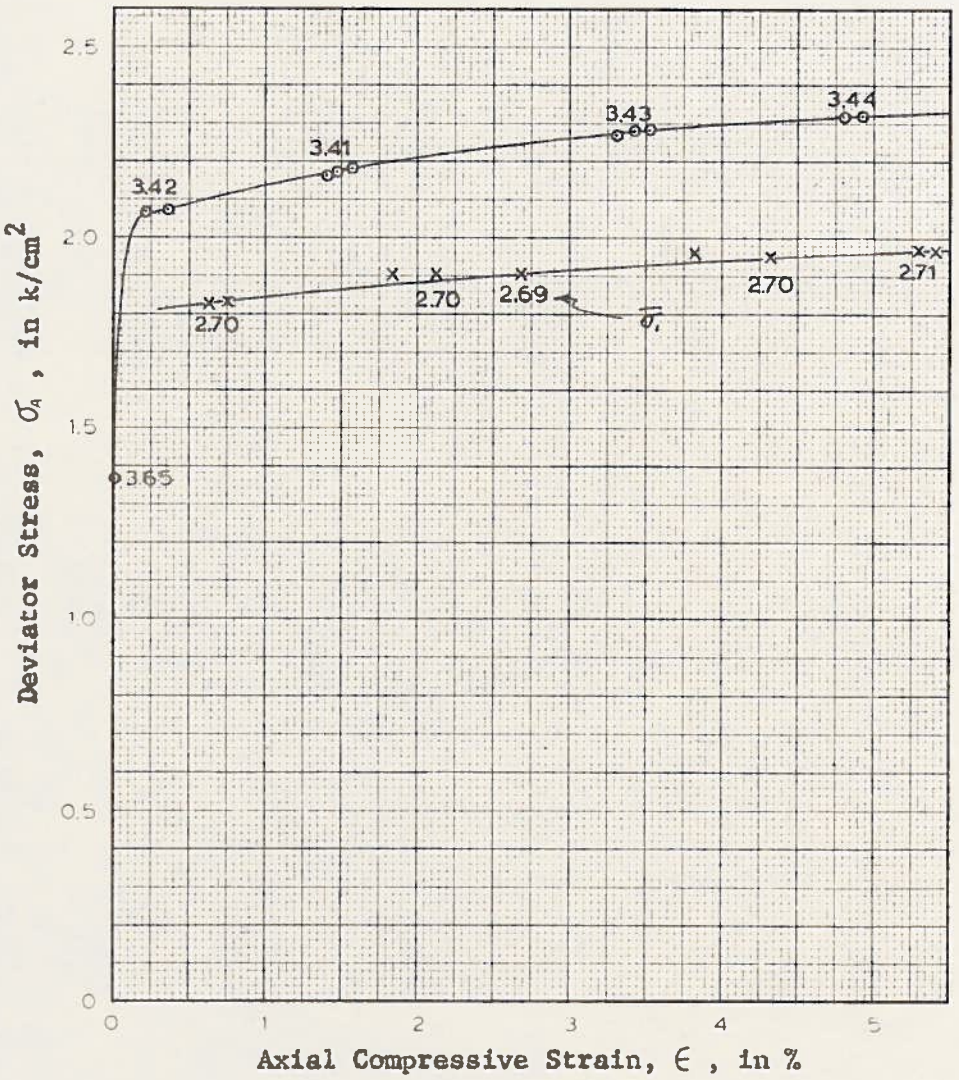

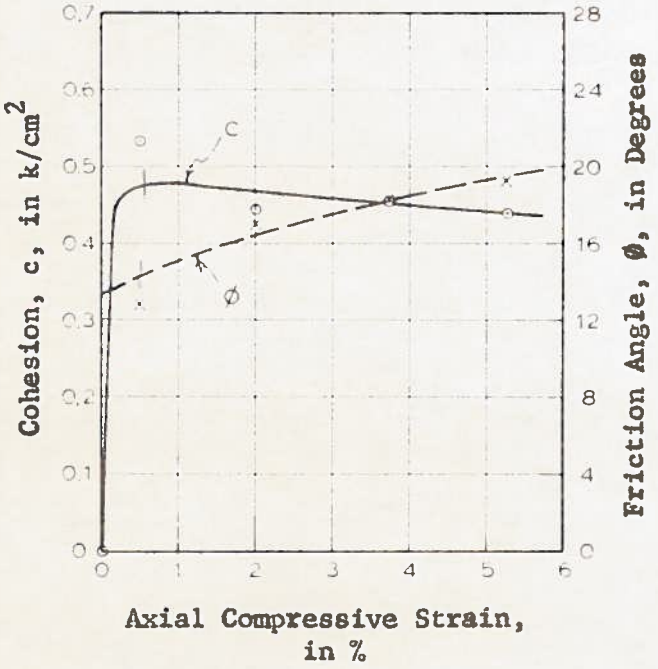

Fig. 22.--Stress-strain curves and computed results for test H-26

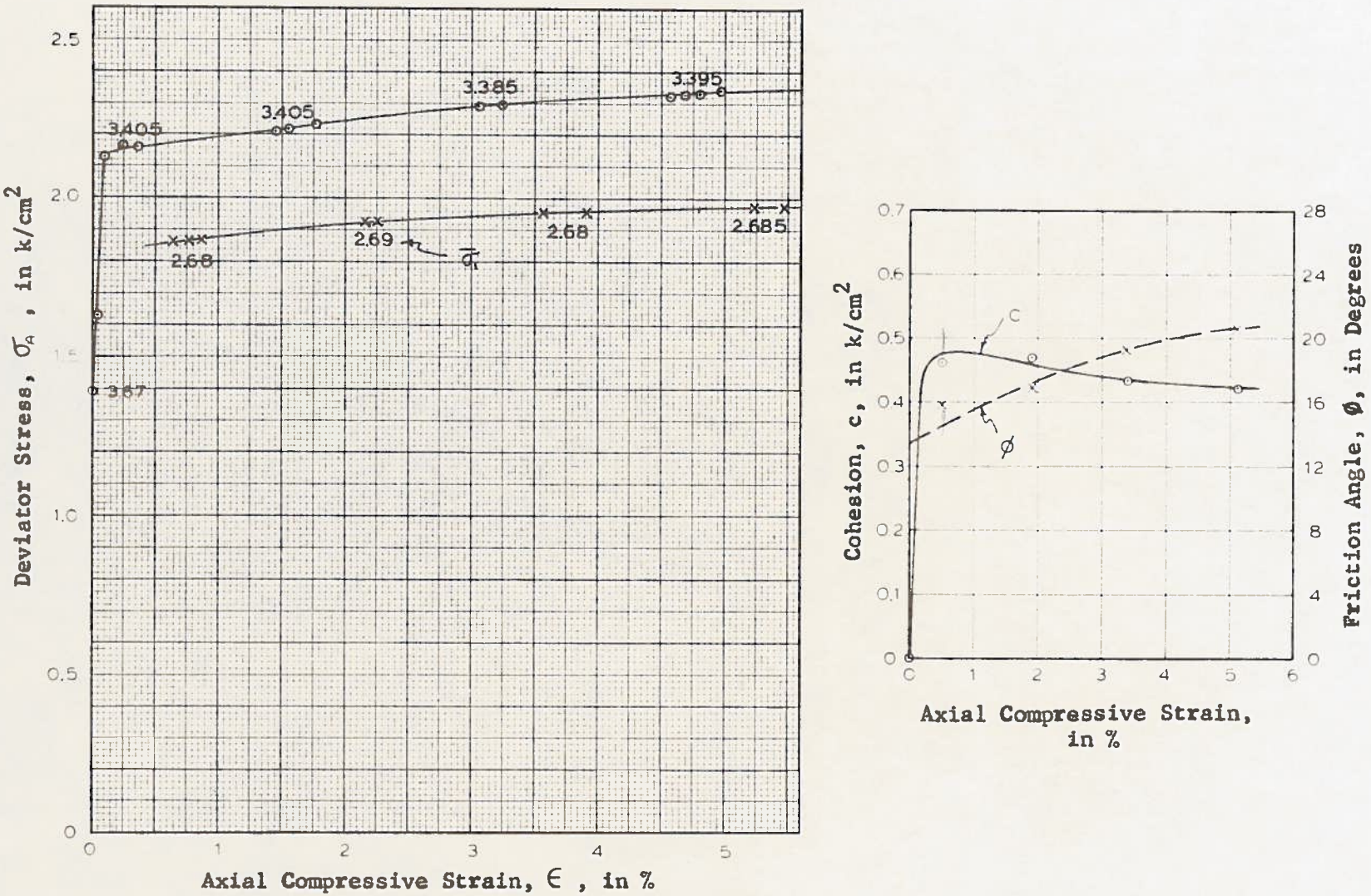

Fig. 23.--Stress-strain curves and computed results for test H-29

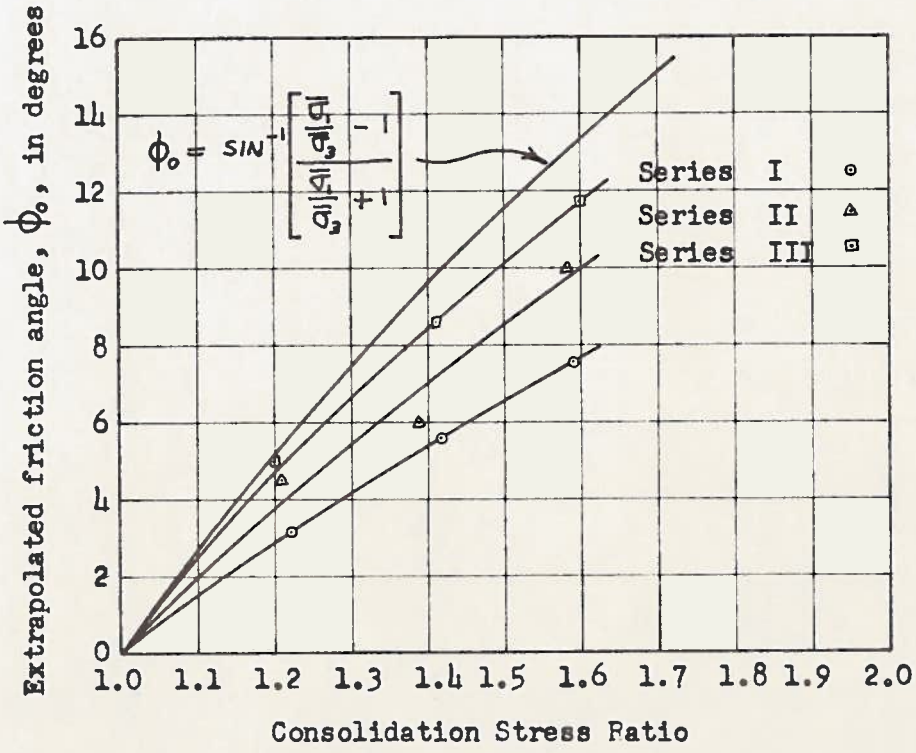

Fig. 24.--Friction angle at zero strain vs. consolidation stress ratio

Tests H-26, H-29 and H-20 were allowed to stand for 66, 131 and 299 hours respectivly after 100% consolidation. From the above observations it is concluded that as the sample proceeds into secondary consolidation the deviator stress is initially carried by both cohesion and friction but is eventually carried totally by friction as the cohesion drops to zero. However, this would only hold true for soils able to develop the required friction to carry the load.

The tests in series I, II and III were carried out after the samples had consolidated between 17.4 and 19.7 hours beyond 100% consolidation. This was insufficient time for the cohesion to drop to zero as seen in figures 18, 19 and 20. The value of ϕ_o vs. consolidation stress ratio is plotted in figure 24 for all three series together with the curve representing the value of friction that would be obtained had the specimens consolidated over an adequate length of time for the cohesion to drop to zero. If cohesion is equal to zero, then,

$$\phi_o = \sin^{-1}\left[\left(\frac{\bar{\sigma}_1}{\bar{\sigma}_3} - 1\right) \div \left(\frac{\bar{\sigma}_1}{\bar{\sigma}_3} + 1\right)\right]. \qquad (3)$$

The required time for the cohesion to drop to zero seems to depend upon the maximum principal stress as well as the type of clay.

Series V. Tests H-27 and H-28 were consolidated as described above to determine the effect of the method used to arrive at the final intergranular stresses. These tests

are shown in figures 25 and 26. There is no significant difference between the results computed from these tests and tests H-26 and H-29, except for the lower value of friction which is caused from the fact that insufficient time was allowed for the cohesion to drop to zero. Considering the vast differences in the method used to consolidate the samples it is concluded that the method of consolidation has no effect on the cohesion and friction of the clay tested. However, it does have an effect on the amount of axial strain that takes place during consolidation.

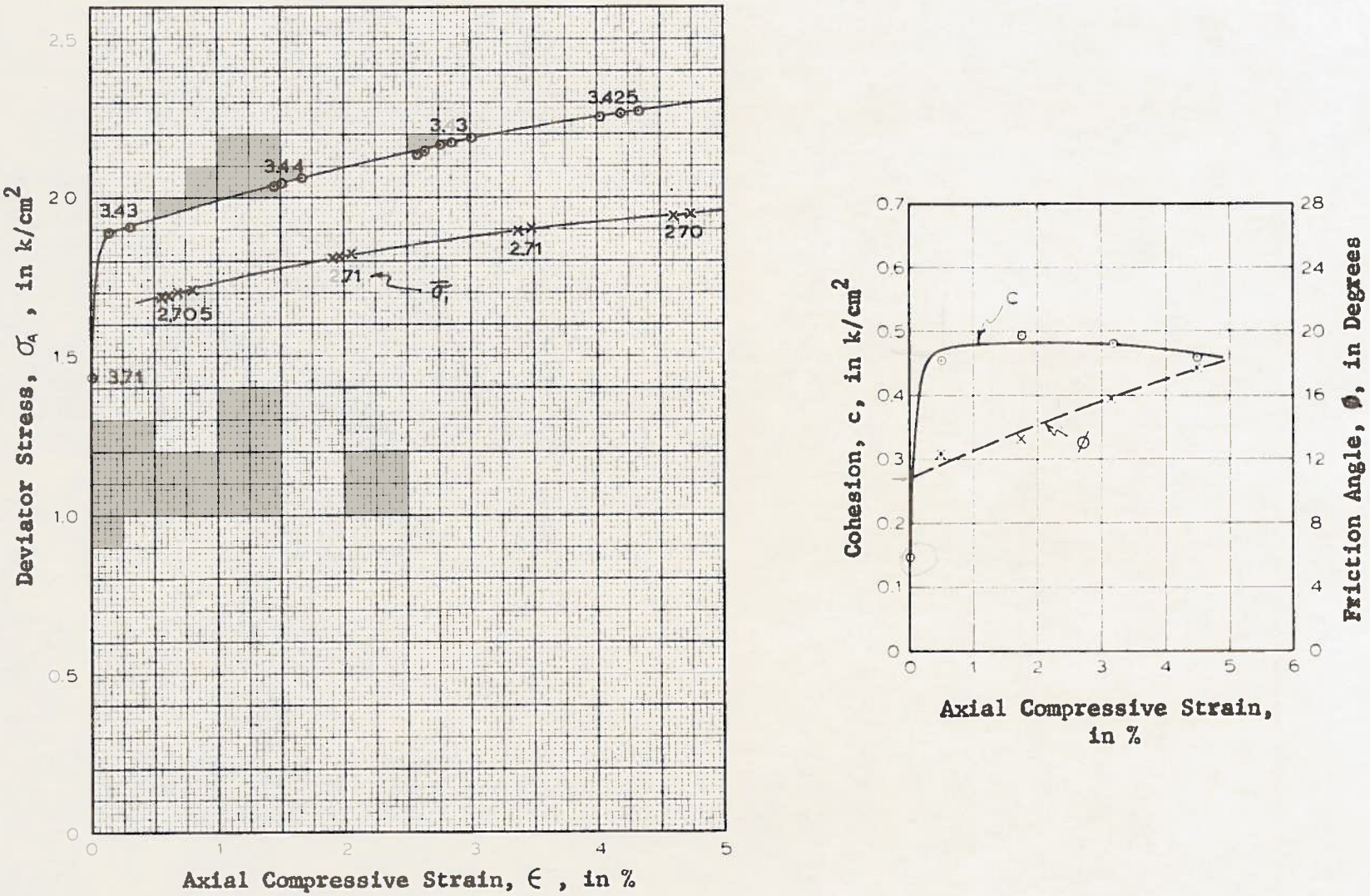

Fig. 25.--Stress-strain curves and computed results for test H-27

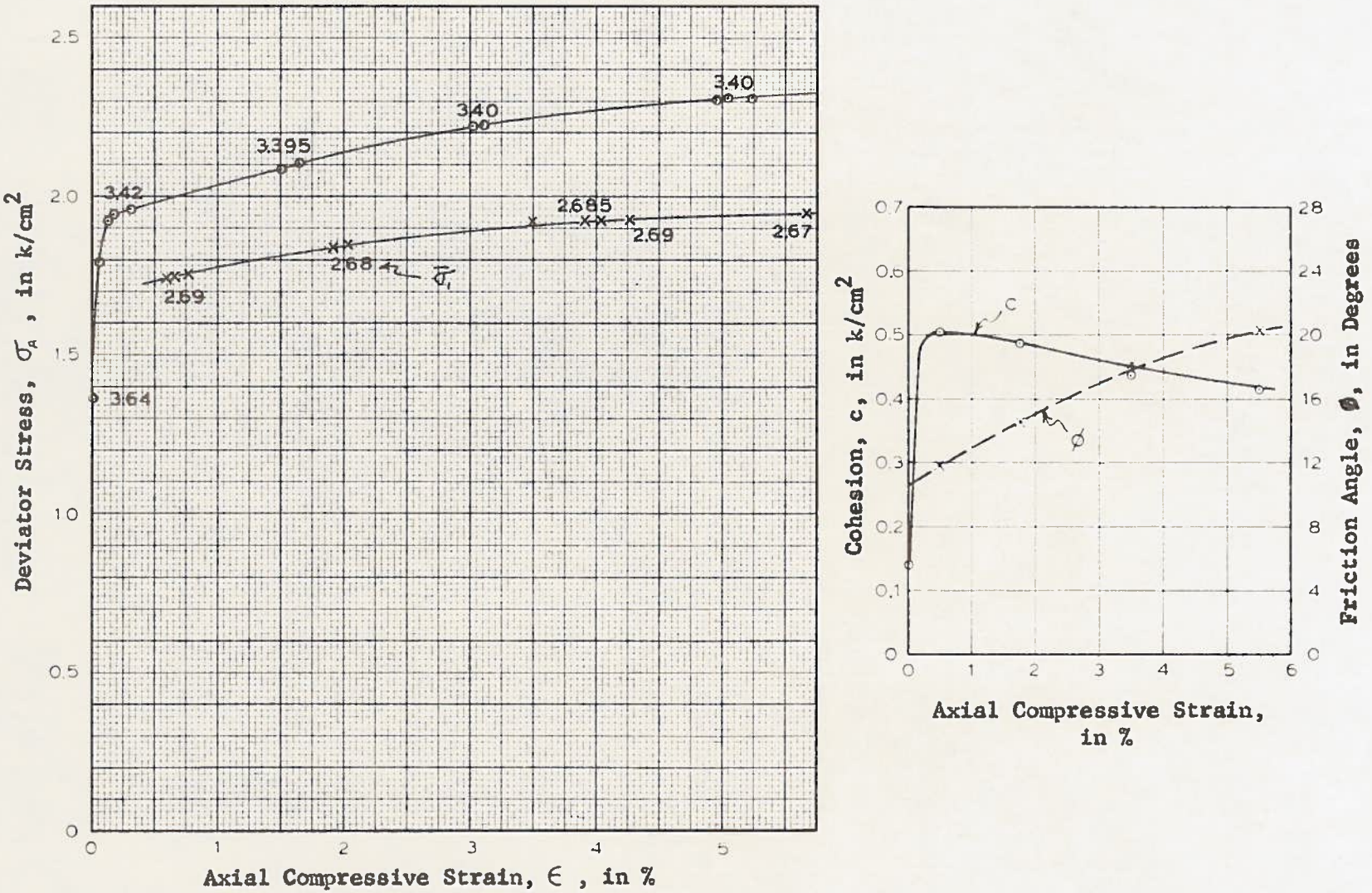

Fig. 26.--Stress-strain curves and computed results for test H-28

SECTION VI

CONCLUSIONS

The following is a summary of the conclusions in regard to anisotropical consolidation and its effect on cohesion and friction in this experimental study.

1. The amount of volume change during consolidation is a function of the maximum principal intergranular stress and is independent of the minor principal stress.
2. At constant rate of strain the peak cohesion is a function of the maximum intergranular stress during consolidation and is independent of the minor principal stress.
3. The value of friction at zero strain is increased by an increase of the consolidation stress ratio, $\left(\frac{\bar{\sigma}_1}{\bar{\sigma}_3}\right)_c$, but varies with strain as it does in a hydrostatically consolidated sample.
4. If the sample is consolidated anisotropically, the initial deviator stress is carried at first by both cohesion and friction but cohesion eventually drops to zero and the total load is carried by friction.

5. The method of consolidating anisotropically does not affect the properties of cohesion and friction. However, it does affect the amount of axial strain that takes place during consolidation.

APPENDIX

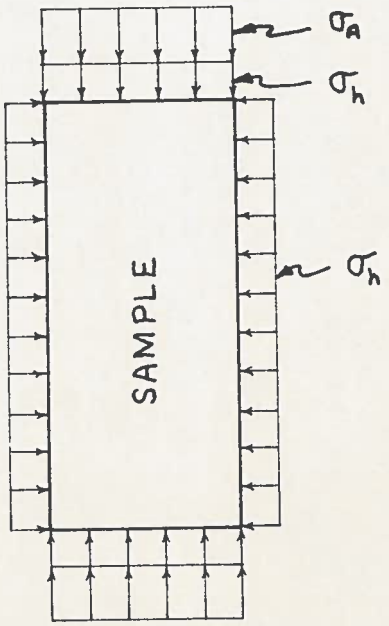

σ_h = CELL PRESSURE

σ_A = STRESS FROM PISTON LOAD

$\sigma_1 = \sigma_A + \sigma_h$

$\sigma_3 = \sigma_h$

Fig. 27.—Stresses imposed on a sample in the triaxial cell

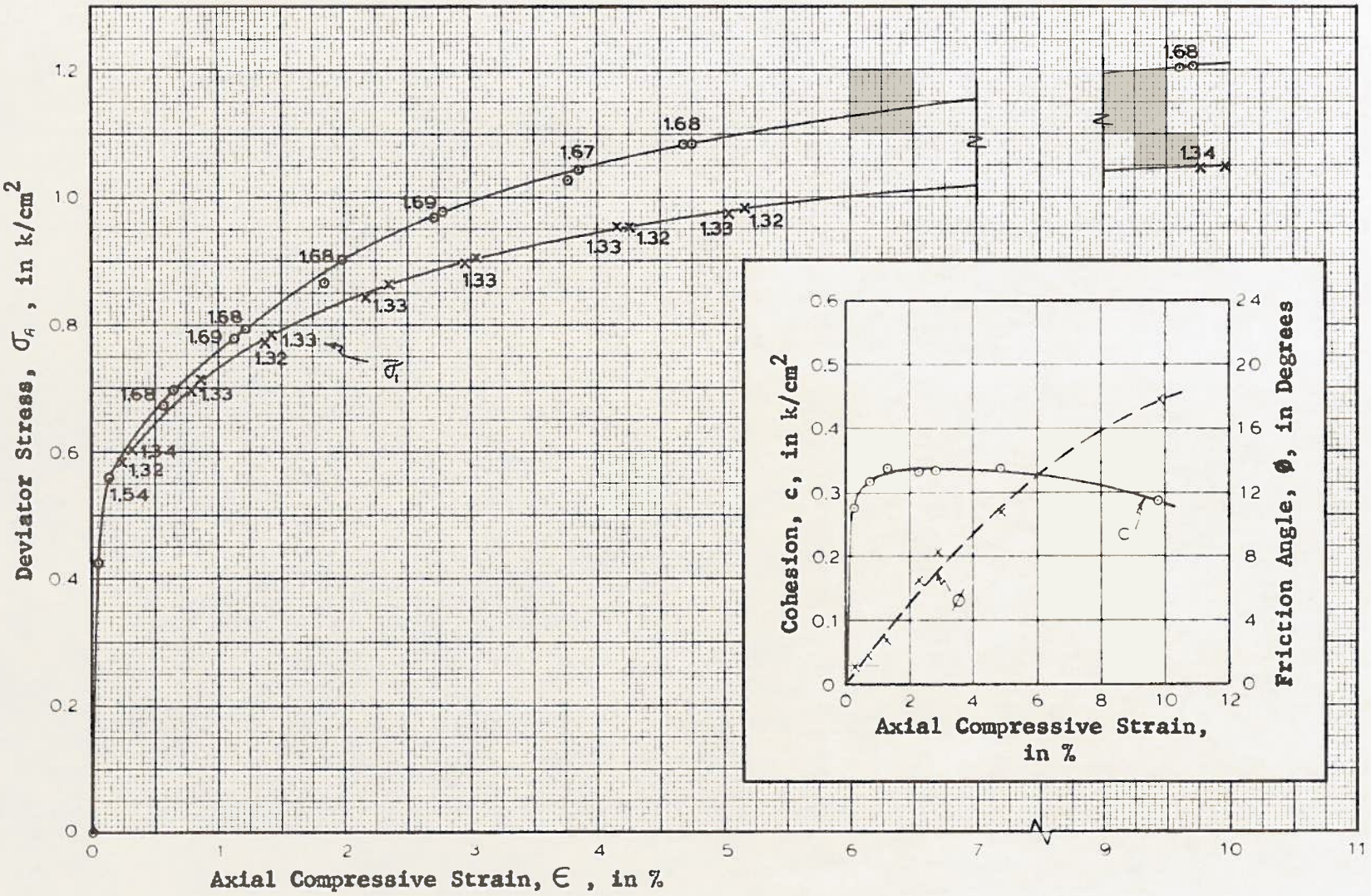

Fig. 28.--Stress-strain curves and computed results for test H-17

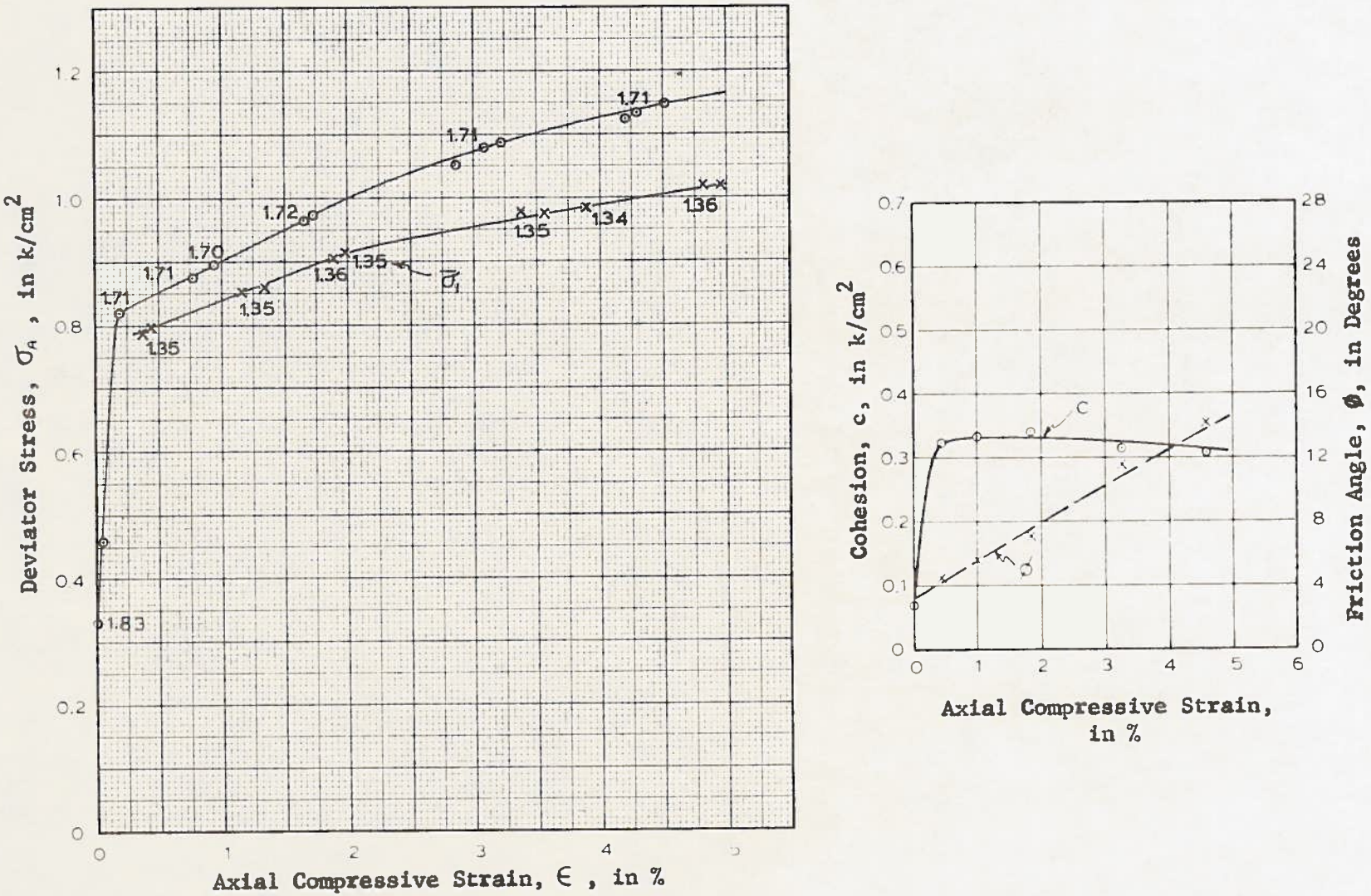

Fig. 29.--Stress-strain curves and computed results for test H-18

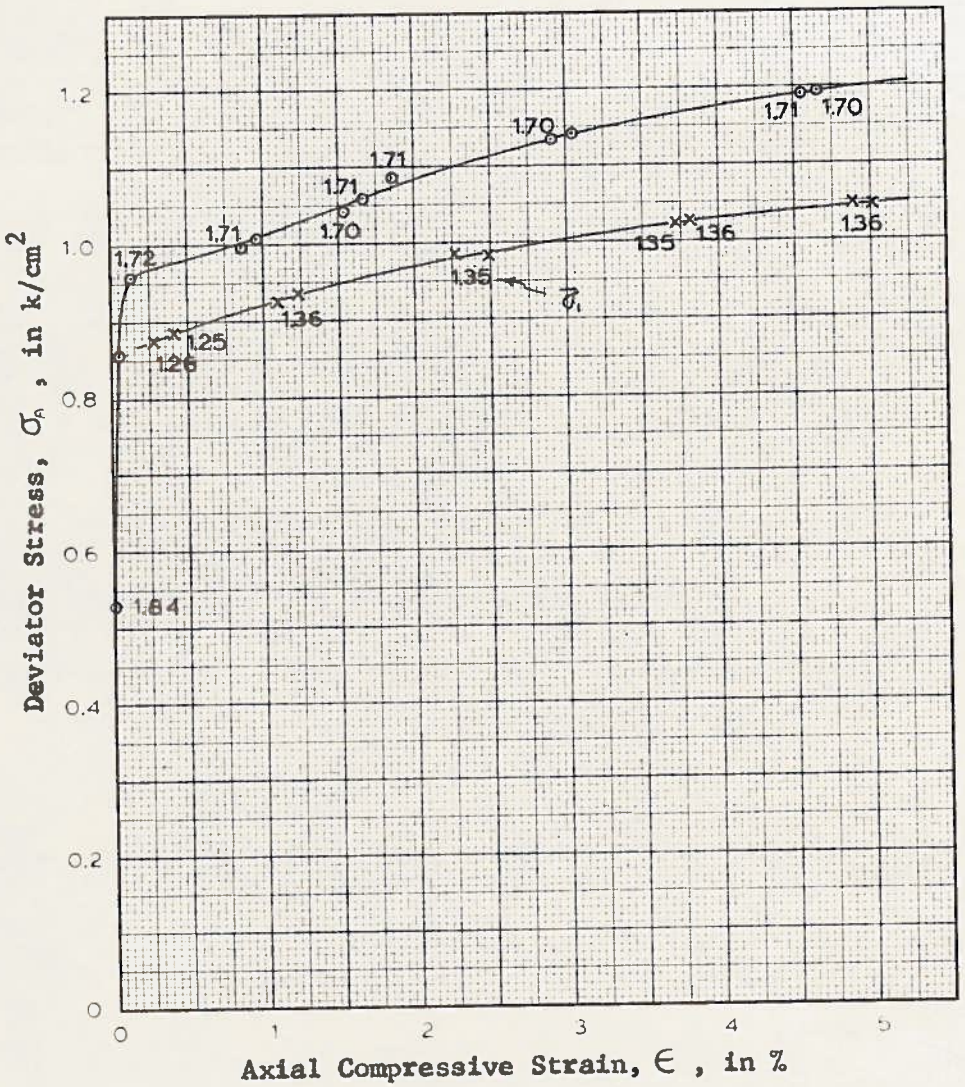

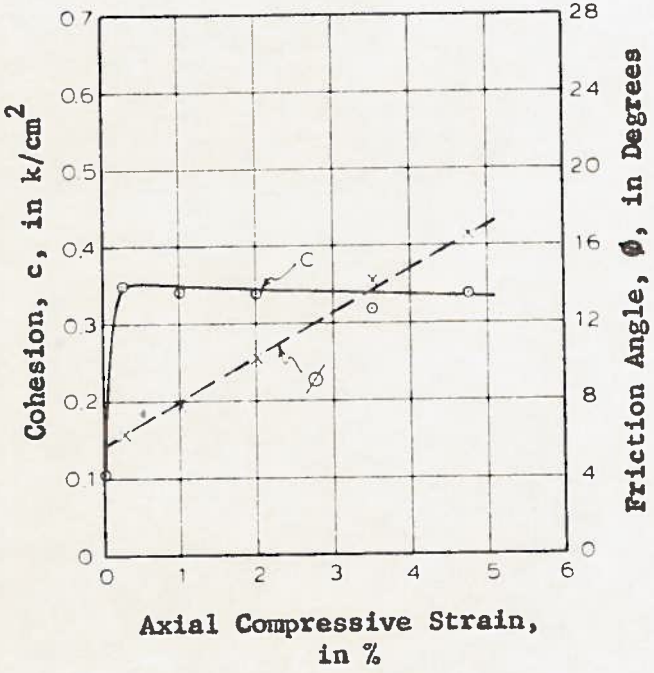

Fig. 30.--Stress-strain curves and computed results for test H-19

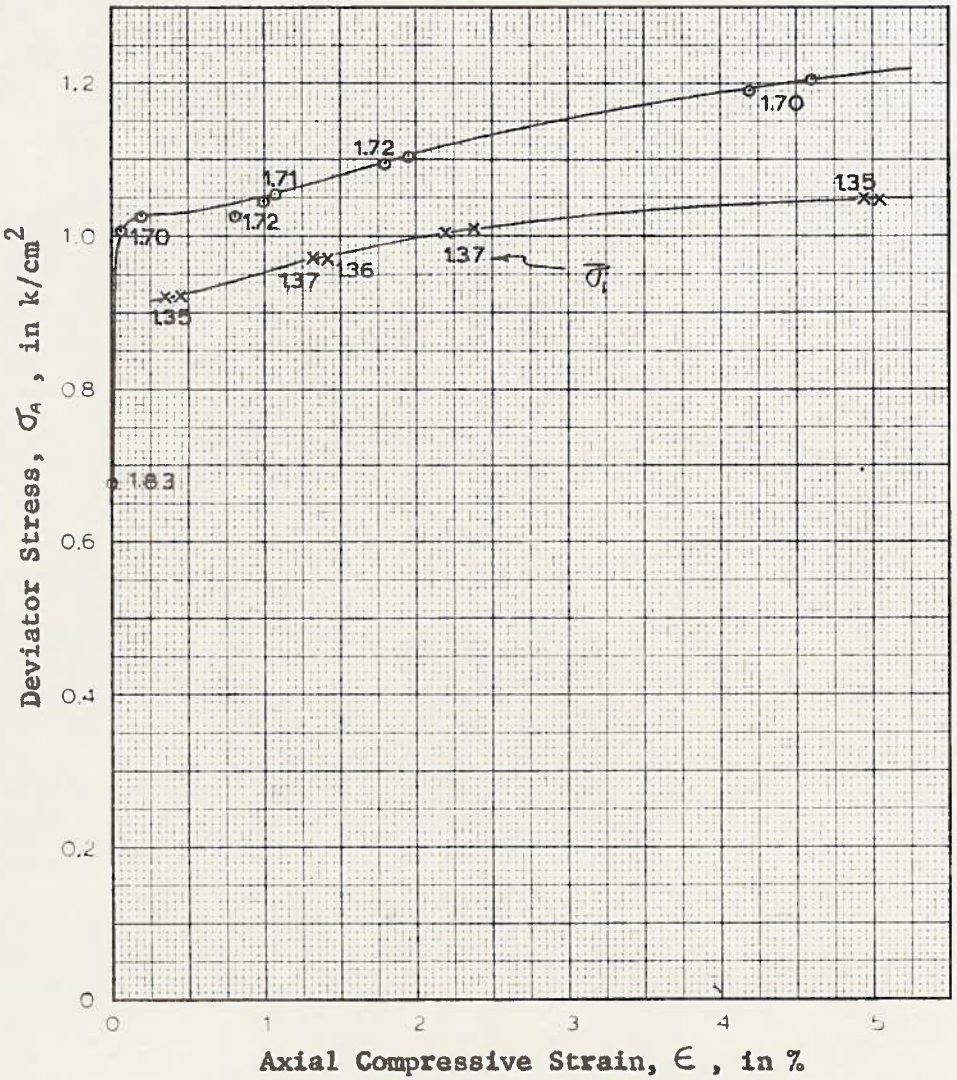

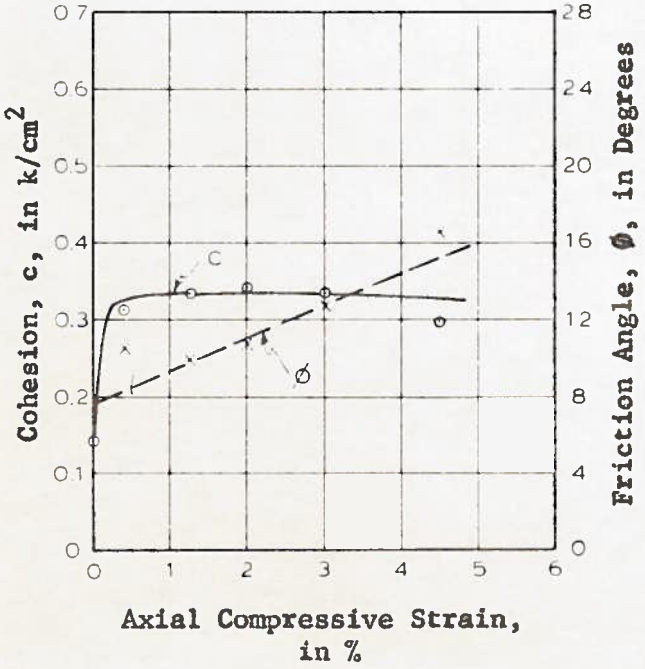

Fig. 31.--Stress-strain curves and computed results for test H-21

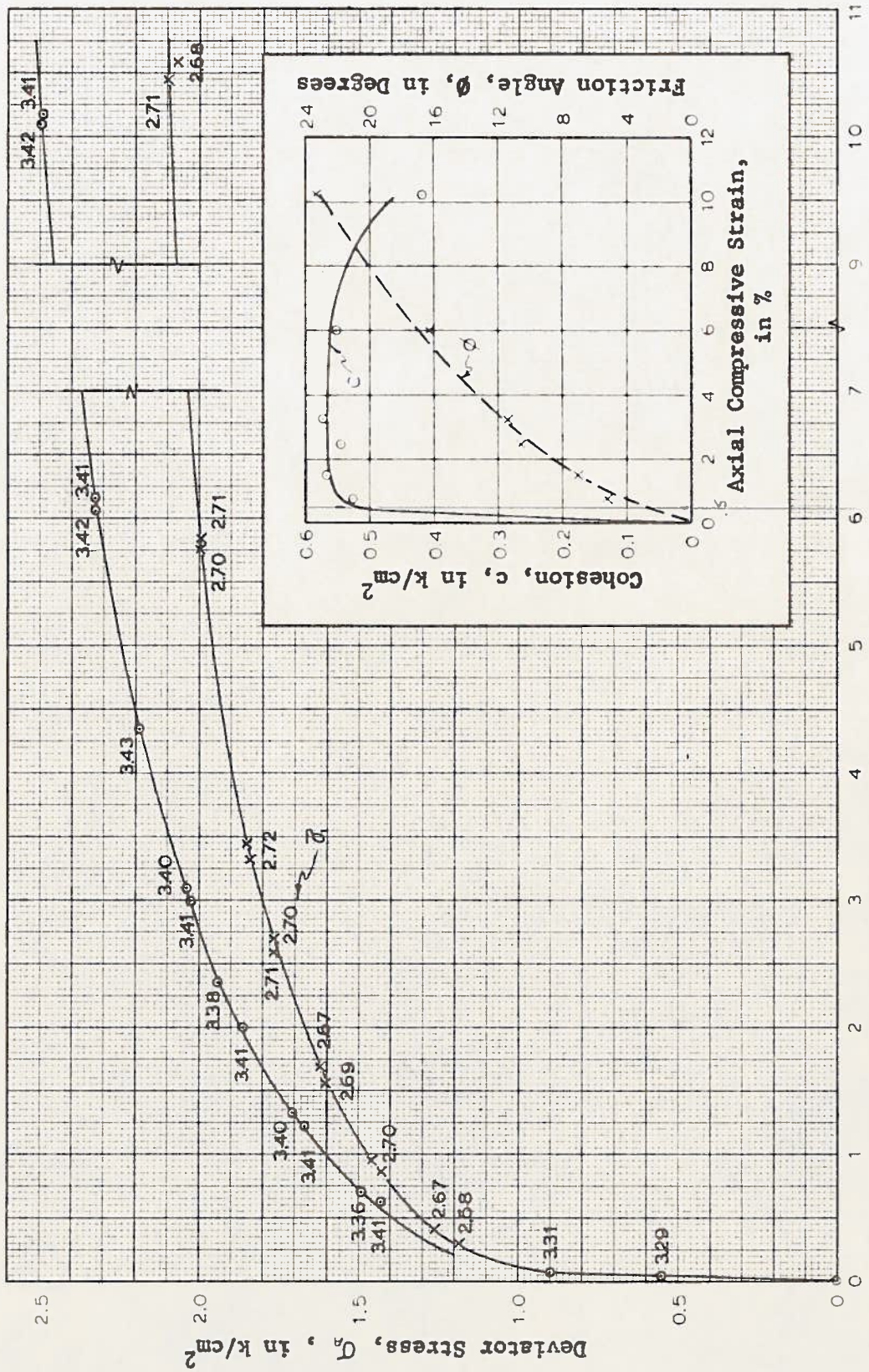

Fig. 32.--Stress-strain curves and computed results for test H-13

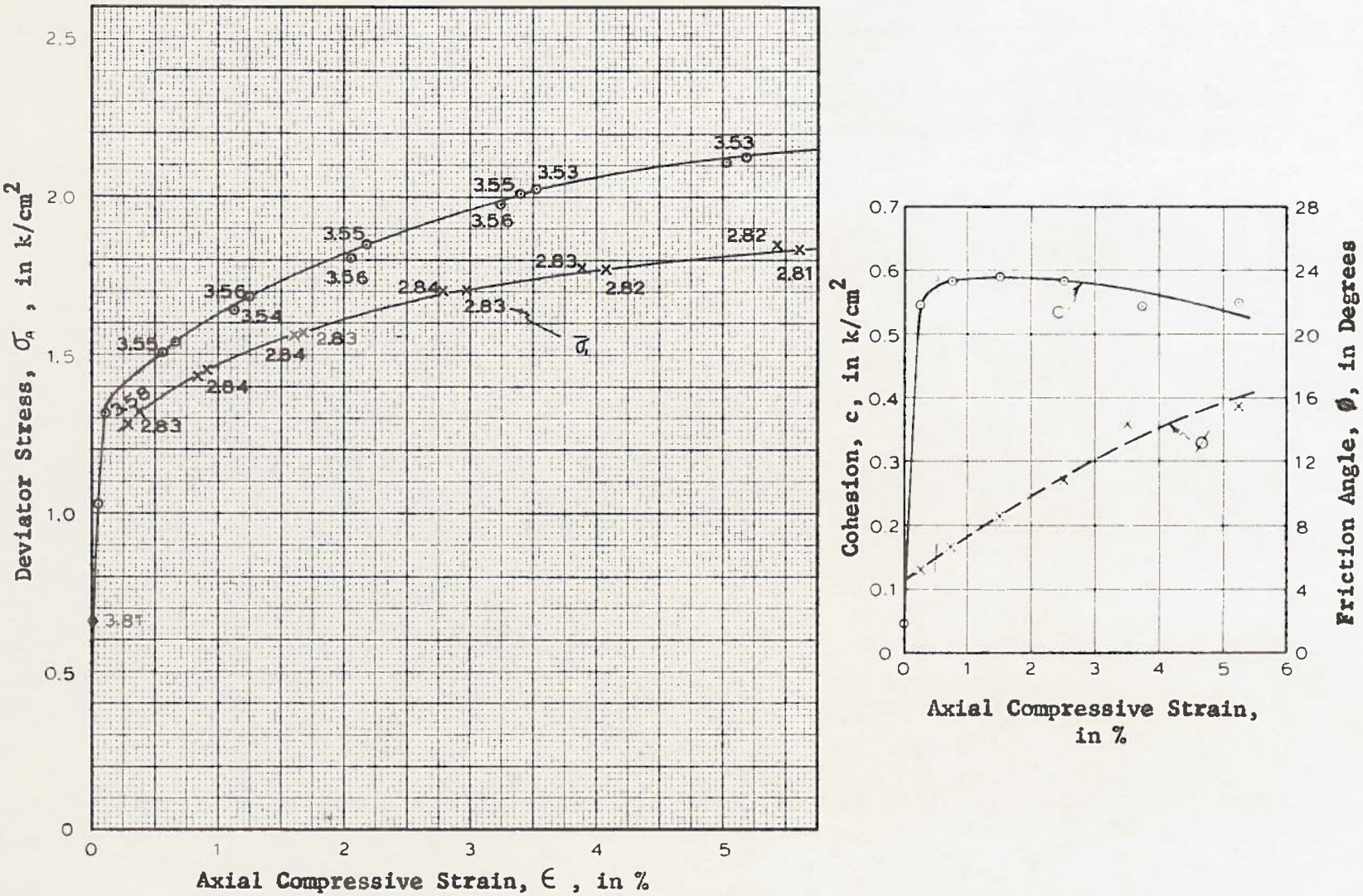

Fig. 33.--Stress-strain curves and computed results for test H-14

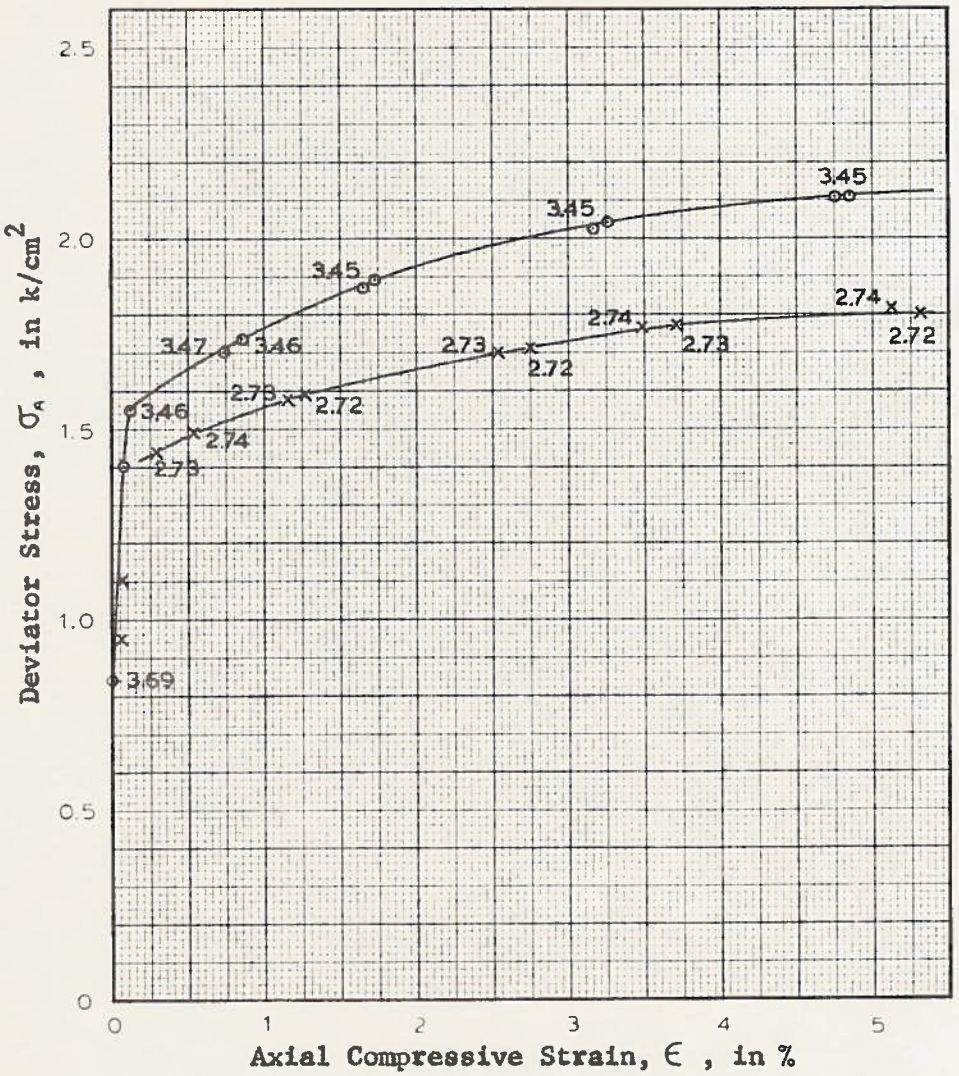

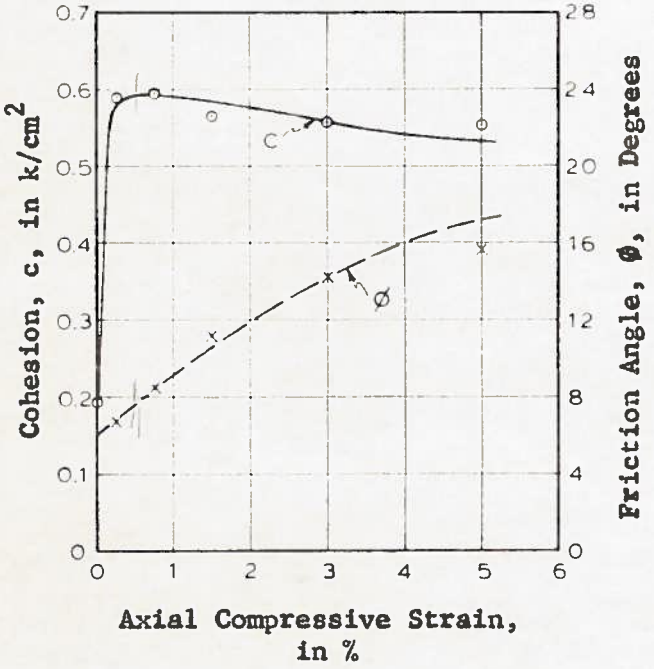

Fig. 34.--Stress-strain curves and computed results for test H-15

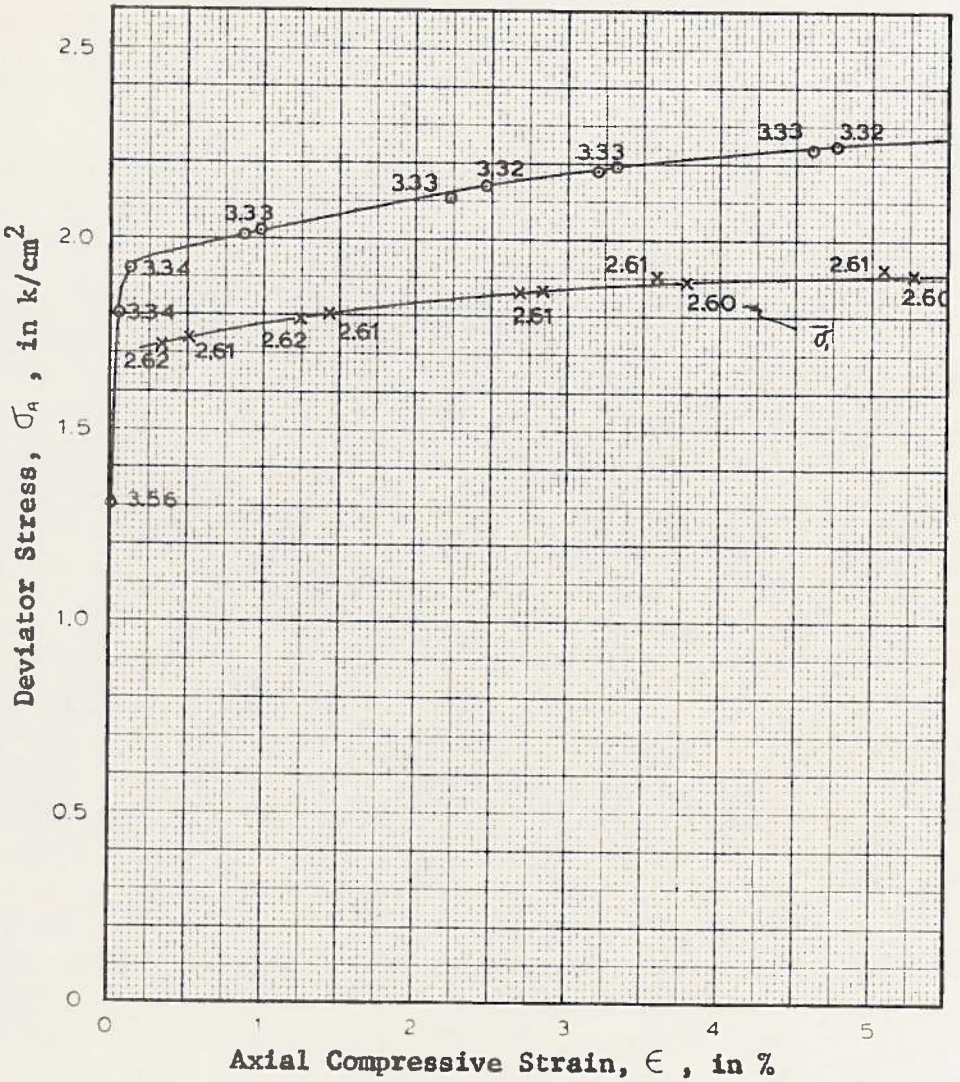

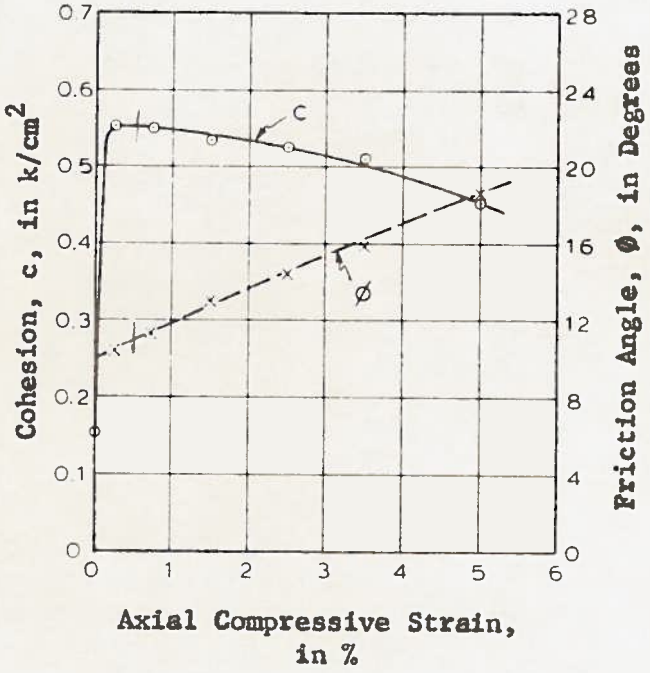

Fig. 35.--Stress-strain curves and computed results for test H-16

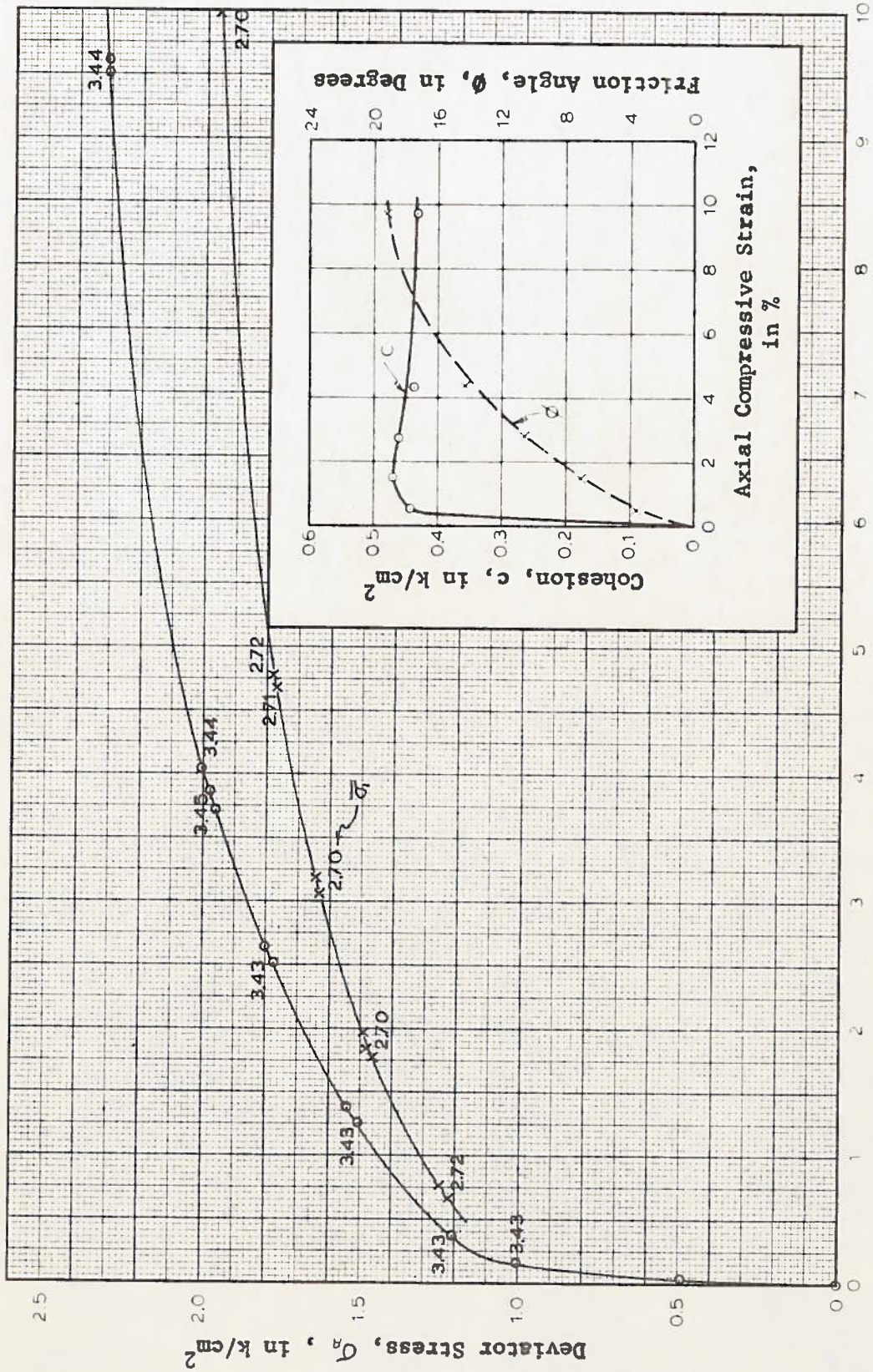

Fig. 36.--Stress-strain curves and computed results for test H-22

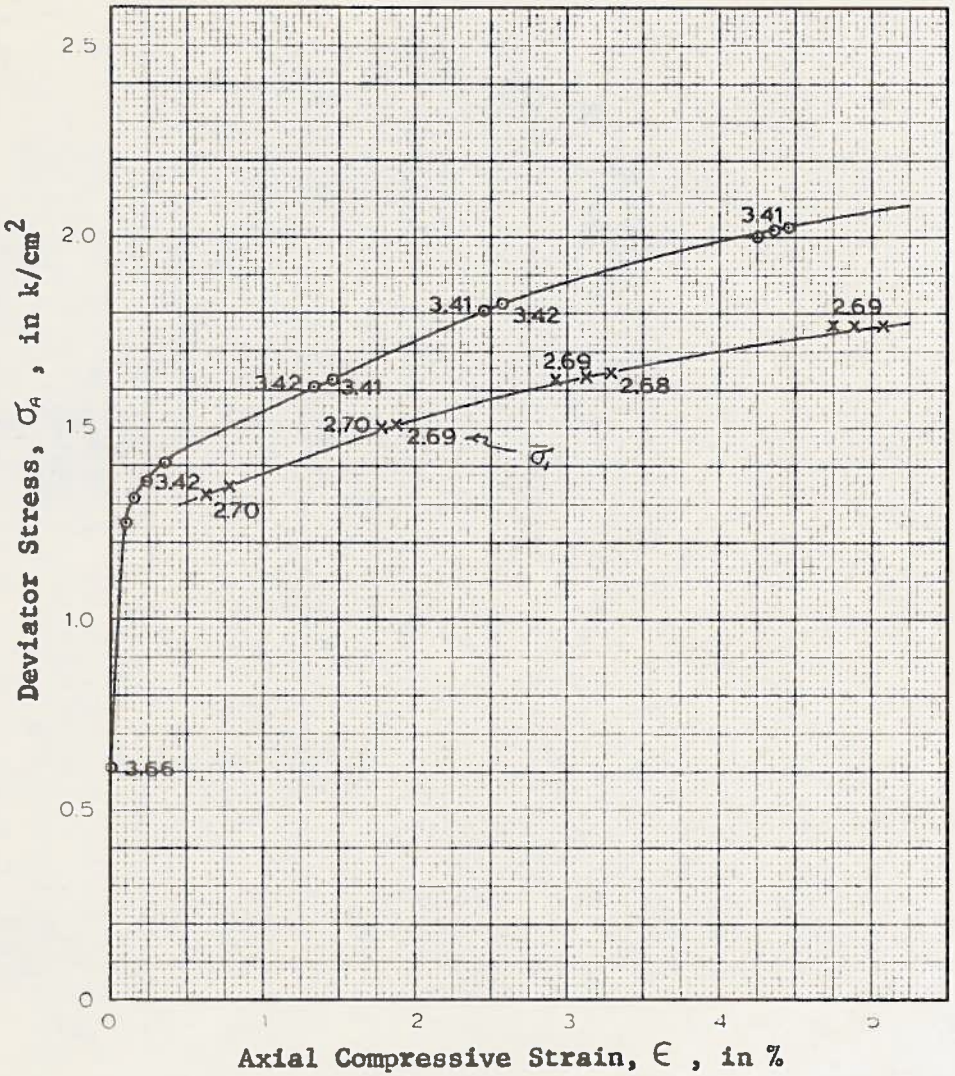

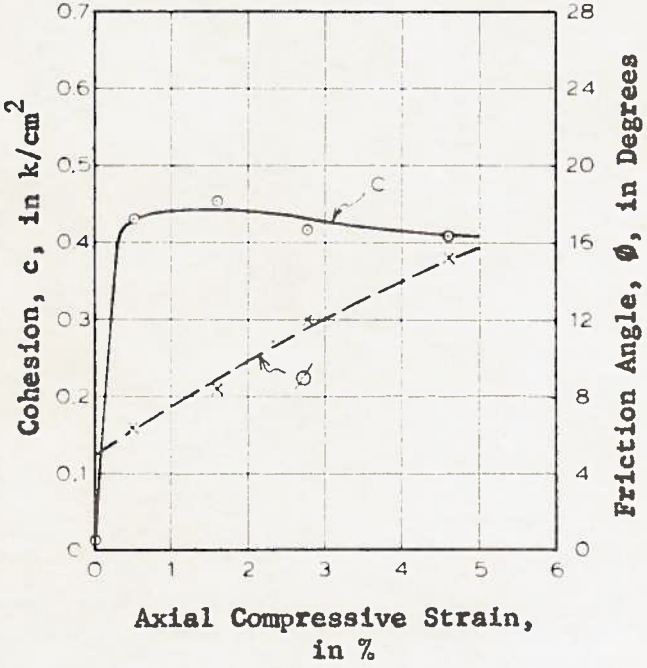

Fig. 37.--Stress-strain curves and computed results for test H-23

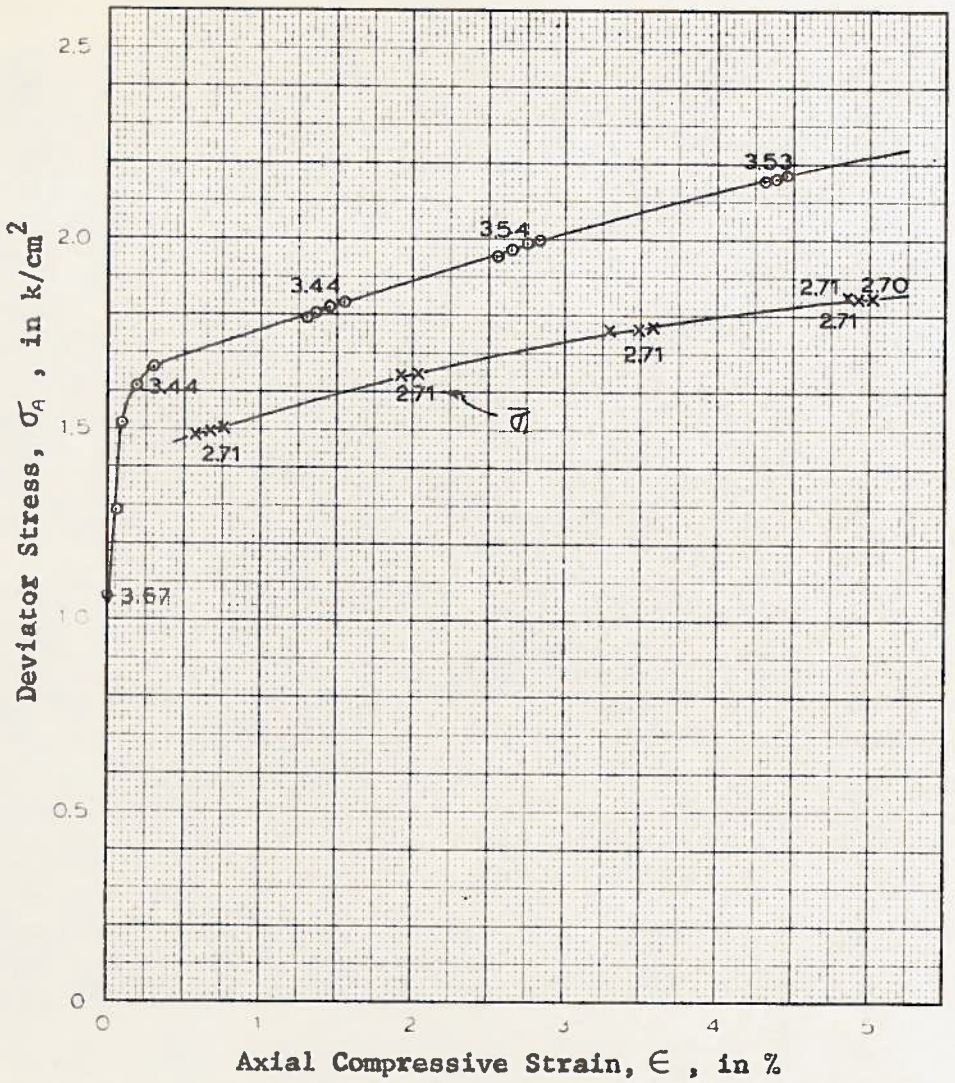

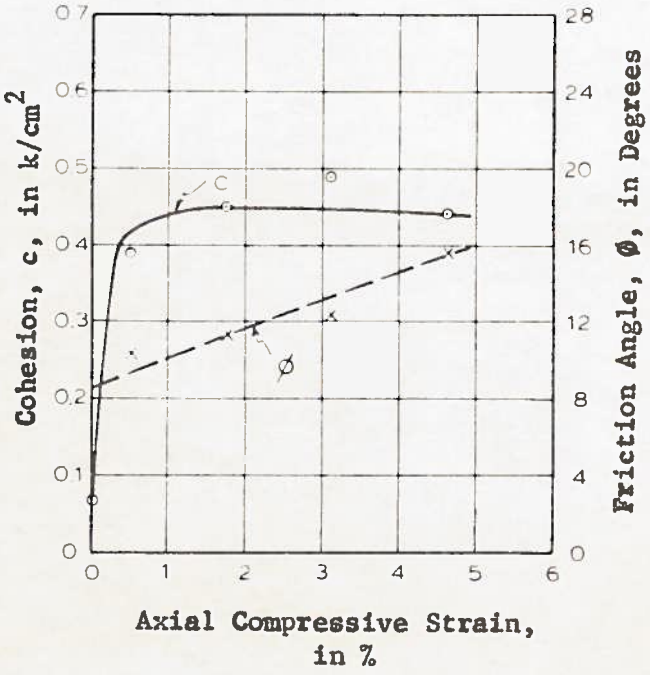

Fig. 38.--Stress-strain curves and computed results for test H-24

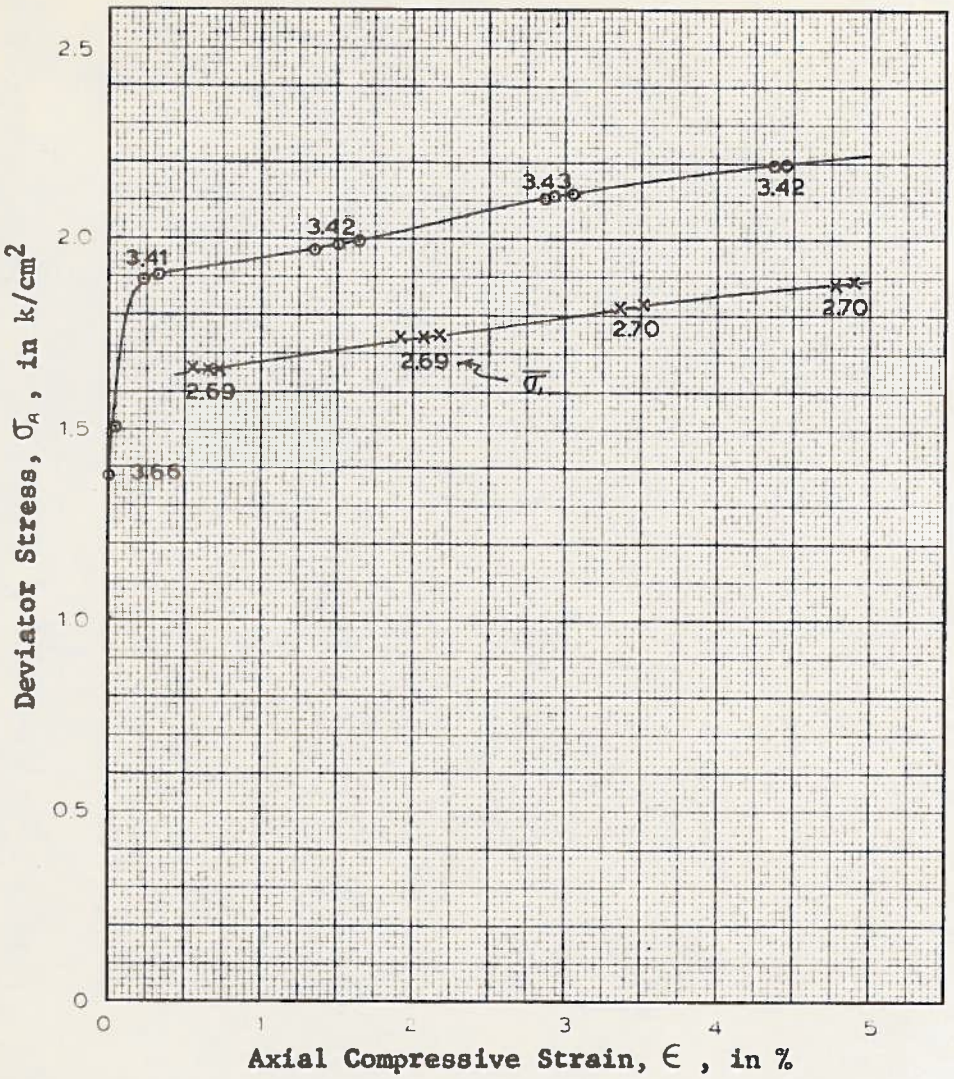

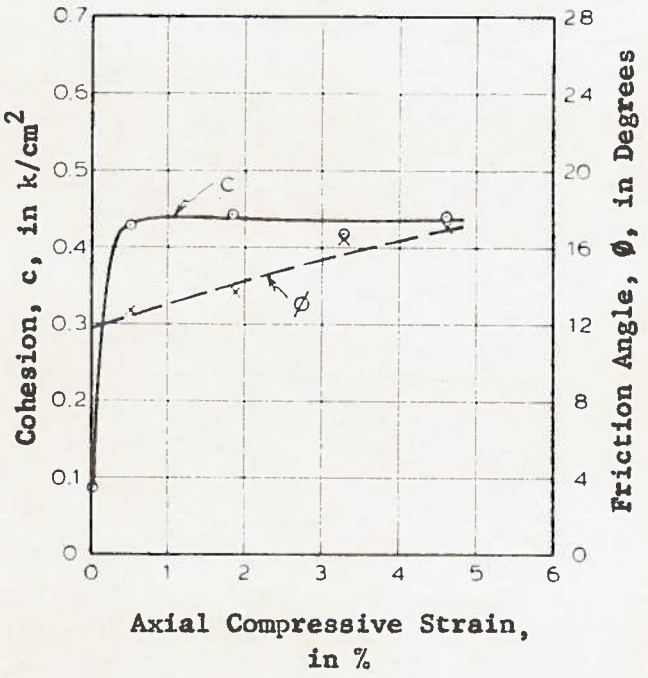

Fig. 39.—Stress-strain curves and computed results for test H-25

LIST OF REFERENCES

1. Bishop, A. W., "Summarized Proceedings of a Conference on Stress Analysis," British Journal of Applied Physics, Vol. I, London: The Institute of Physics, October, 1950.

2. Bishop, A. W., and Eldin, A. K. G., "Undrained Triaxial Tests on Saturated Sands and their Significance in the General Theory of Shear Strength," Geotechnique, Vol. II, No. 1. London: The Institution of Civil Engineers, 1950.

3. Whitman, R. V., "Some Considerations and Data Regarding the Shear Strength of Clays," Preprint of the Research Conference on the Shear Strength of Cohesive Soils, American Society of Civil Engineers, Boulder, Colorado, June, 1960.

4. Bjerrum, L., "Theoretical and Experimental Investigations on the Shear Strength of Soils," Norwegian Geotechnical Institute Publication No. 5, Oslo, 1954.

5. Schmertmann, J. H., and Osterberg, J. O., "An Experimental Study of the Development of Cohesion and Friction with Axial Strain in Saturated Cohesive Soils," Preprint of the Research Conference on the Shear Strength of Cohesive Soils, American Society of Civil Engineers, Boulder, Colorado, June, 1960.

6. Andresen, A., Bjerrum, L., DiBiago, E., and Kjaernsli, B., "Triaxial Equipment Developed at the Norwegian Geotechnical Institute," Norwegian Geotechnical Institute Publication No. 21, Oslo, 1957.

7. Matlock, H., Jr., Fenske, C. W., and Dawson, R. F., "De-Aired, Extruded Soil Specimens for Research and for Evaluation of Test Procedures," ASTM Bulletin No. 177, October, 1951.

8. Rutledge, P. C., "Cooperative Triaxial Shear Research Program of the Corps of Engineers," Soil Mechanics Fact Finding Survey, Progress Report, Waterways Experiment Station, Vicksburg, Mississippi, April, 1947.

9. MacFarlane, J. W., "Effect of Structure on Secondary Compression of Kaolinite," Unpublished Master's thesis, College of Engineering, University of Florida, 1959.

10. Terzaghi, K., "Settlement of Pile Foundations due to Secondary Compression," Proceedings of the Fourth Texas Conference on Soil Mechanics and Foundation Engineering, The University of Texas, Austin, February, 1941.

BIOGRAPHICAL SKETCH

John Russell Hall, Jr. was born in Orlando, Florida, on September 19, 1936. In June, 1954, he graduated from Mount Lebanon High School in Pittsburgh, Pennsylvania. In January, 1959, he received the degree of Bachelor of Civil Engineering from Syracuse University.

He was employed two summers by Westinghouse Electric Corporation in East Pittsburgh, Pennsylvania, and two other summers by Harrison Construction Company. He worked as a graduate research assistant in the Department of Civil Engineering for three semesters at the University of Florida.

He is a member of Tau Beta Pi and an Associate Member of ASCE.

This thesis was prepared under the direction of the chairman of the candidate's supervisory committee and has been approved by all members of that committee. It was submitted to the Dean of the College of Engineering and to the Graduate Council, and was approved as partial fulfillment of the requirements for the degree of Master of Science in Engineering.

June 6, 1960

_____
Dean, College of Engineering

_____
Dean, Graduate School

SUPERVISORY COMMITTEE

_____
Chairman

_____

_____

_____